UNIVERSITY POLITEHNICA OF BUCHAREST

Faculty of Applied Chemistry and Materials Science

Department Analytical Chemistry and Environmental Engineering

The Senat Decision No. 364/28.03.2019

PhD THESIS SUMMARY

APPLICATIONS OF SOME CARBON NANOSTRUCTURES AS SORBENTS FOR INORGANIC CONTAMINANTS

Author: chem. **Luiza Ciupercă (Capră)**

PhD Supervisor: Prof. PhD. eng. **Alina Catrinel Ion**

EXAMINATION BOARD

Head of examination board	Prof. PhD. eng. Vasile Lavric	from	University POLITEHNICA of Bucharest
PhD Supervisor	Prof. PhD. eng. Alina-Catrinel Ion	from	University POLITEHNICA of Bucharest
Referent	Academician Maria Zaharescu	from	Romanian Academy
Referent	Prof. Emeritus Aurelia Meghea	from	University POLITEHNICA of Bucharest
Referent	Prof. PhD. chem. Victor David	from	University of Bucharest

Bucharest
-2019-

CUPRINS

*The content respects the pagination in the doctoral thesis. Also, the selected experimental part maintains the order of the thesis; the numbers of the figures, the tables, the equations and the bibliographic sources in this abstract correspond to the numbering of those in the doctoral thesis.

INTRODUCTION

According to the current scientific community's concerns to find solutions to eliminate inorganic contaminants in natural waters with the help of nanotechnology, the present thesis proposed the study of Sb (III) adsorption on oxidized graphite exfoliated nanoplates (ox-xGnP).

Natural water is a vital element for human life and health. Therefore, it is very important for it to be devoid of heavy metals which can cause various diseases in human body [3]. The toxicity of antimony and its compounds has been of increased concern worldwide. Antimony (Sb) is a toxic element even at very low concentrations. In general, inorganic antimony is more toxic than organic antimony. The compounds of Sb (III) are 10 times more toxic than those of Sb (V) [4]. Exposure to 9 mg of antimony per cubic meter of air over a long period of time causes irritation of the eyes, skin and lungs. Inhalation of 2 mg of antimony per cubic meter of air in humans can cause problems with the lungs (pneumoconiosis) and heart (modified electrocardiogram), stomach pain, diarrhea, vomiting and gastric ulcer. Antimony may also induce the following conditions: dermatitis, keratitis, conjunctivitis.

Keywords: oxidized exfoliated graphite nanoplatelets, adsorption, sorption, Sb, environmental contaminants, natural waters.

The research in this doctoral thesis aimed at the study of Sb (III) adsorption on oxidized graphite exfoliated nanoplates (ox-xGnP) in order to evaluate the potential of ox-xGnP as an adsorbent for Sb (III).

The research study on the status of research into the type of inorganic contaminants present in natural waters, such as carbon nanomaterials currently used as sorbents, and the existing methods of analysis for the determination of Sb has led to the setting of the following objectives for the fulfilment of the thesis' proposed purpose:

- development, optimization and validation of determination methods of Sb in drinking water, natural mineral water and PET;
- characterization of ox-xGnP before and after adsorption of Sb (III);
- study of the influence of adsorption parameters: the pH of the solutions, the amount of ox-xGnP, the contact time, the initial concentration of Sb (III) and the temperature;
- adsorption kinetics study of the process;
- study of adsorption isotherms of the process;
- the study of thermodynamic parameters;

- proposed mechanism for adorption of Sb (III) onto ox-xGnP;
- adsorption of Sb (III) on ox-xGnP from different types of water.

The thesis is structured in two main parts, a theoretical part comprising three chapters and an experimental one organised in two chapters. The theoretical part is structured in three chapters as follows:

Chapter 1 of the thesis presents the current state of the carbon nanomaterials, their classification according to their structure and the different morphologies they present. The structure, properties, methods of obtain and applications in different fields, Fullerene, carbon nanotubes and graphite are presented in more detail. Also, there are presented the methods for obtaining the exfoliated nanoplatelets graphite. This chapter also presents the characterization techniques of carbon nanomaterials with the advancements and limitations of each. The chapter ends with an example of the various possibilities of carbon nanomaterials applications, detailing their use as sorbents for metal ions. In this respect, comparative literature data on the adsorption of several heavy metal contaminants on different types of adsorbents are presented. The last subchapter highlights the fact that there is little research on Sb adsorption on carbon nanomaterials.

Chapter 2 presents the theoretical aspects of the adsorption phenomens, the adsorption types and the adsorption isotherms that underlie the mechanisms that shape the adsorption process. There are described the most common isothermal equations applied, such as Langmuir and Freundlich and other types of isotherms less commonly used in modeling experimental data.

In **Chapter 3** there is a classification of natural waters according to origin and chemical composition. The drinking water quality parameters and types of contaminants are presented, detailing potential sources of contamination with Stibiu.

A research direction presented in the three subchapters of **chapter 4** of the experimental part consisted in the development methods for Sb determination by inductively coupled plasma optical emission spectrometry (ICP-OES) in drinking water and mineral waters, as well as developing and optimazing a method of Sb determination from polyethylene terephthalate, based on an original digestion method. In the chapter, the description of the used equipment, the way of working, the parameters of the studied performance as well as the obtained results are presented in a detailed way. The three developed methods show satisfactory performance, comparable to other techniques presented in the literature.

Chapter 5 presents the experimental results of the adsorption study of Sb (III) on oxidized exfoliated nanoplatelets graphite (ox-xGnP). ox-xGnP was characterized before and after adsorption by techniques such as TGA, FT-IR, BET, SEM and TEM STEM / EDX. The

study of the influence of adsorption parameters to optimize the sorption process comprised the influence of pH, ox-xGnP concentration, contact time, initial concentration of Sb (III) and temperature. It also presents the study of kinetics, adsorption isotherms and thermodynamic parameters of the adsorption process. The chapter ends with the proposal of a Sb (III) adsorption mechanism on ox-xGnP and a range of applications from different types of natural waters.

The thesis also includes a chapter of general conclusions in which the main conclusions of the researches carried out are systematized and a section with the original contributions and future directions of research, as well as the list of scientific papers and scientific papers during the doctoral studies are summarized. The bibliography (list of papers reviewed and published) concludes this thesis.

EXPERIMENTAL PART

CHAPTER 4

4. 1. METHOD FOR DETERMINATION OF ANTIMONY IN DRINKING WATER

A method for the determination of Sb in drinking water by inductively coupled plasma optical emission spectrometry (ICP-OES) has been developed using the Optima 2100 DV ICP-OES System Perkin Elmer (Waltham, MA, USA) with both axial and radial viewing plasma configuration operating at a 40 MHz free-running ratio-frequency.

4.1.2. Analysis method

Plasma view mode is axial and spectral line was found at λ=206,836 nm. For the determination of Sb in drinking water the calibration curve was obtained by diluting the stock of 100 mg L^{-1}, Quality Control Standard 21, for preparing calibration standard solutions of: 2,0; 5,0; 10,0; 20,0; 30,0 μg L^{-1}. The solutions were analyzed automatically and the calibration curve was obtained. The drinking water samples were injected and analyzed in the same manner as the standard solutions, then there were processed the results. The operating conditions are shown in Table 9.

Table 9. Operating Conditions for Optima 2100 DV ICP-OES.

No.	Parameter	Unit	Value
1.	RF incident power	kW	1,25
2.	Nebulizer argon flow rate	mL min^{-1}	0,75

3.	Plasma argon flow rate	mL min^{-1}	15
4.	Auxiliary argon flow rate	mL min^{-1}	1,5
5.	The flow rate of the peristaltic pump	mL min^{-1}	1,5
6.	Total time for analysis	sec.	cca. 110

The relevant performance parameters that were studied for this method, published [209], are presented in Table no. 10, together with the acceptance criteria and the maximum admissible concentration (CMA) of the antimony according to the legislation in force.

Table 10. Performance parameters and acceptance criteria

No.	Performance parameters	Unit	The maximum admissible concentration (CMA)	Acceptance criterion	Reference
1.	Liniarity	-	-	$r \geq 0,997$	[210]
2.	Detection limit, LoD	µg L^{-1}	5	1,25	[175]
3.	Quantification limit, LoQ	µg L^{-1}	5	3,75	
4.	Precision (Repeatability)	µg L^{-1}	5	1,25	
5.	Accuracy	µg L^{-1}	5	1,25	
6.	Recovery	%	-	92% ÷ 104%.	[211]

For an average concentration of 11.1 µg L^{-1} and a coverage factor k = 2, corresponding to a confidence level of 95% the expanded uncertainty of the method is 1.7 µg L^{-1} [213].

Based on results obtained from ICP-OES method validation „in house'' (Table 14), it was observed that all acceptance criteria in Table 10 are meet.

Table 14. Results from validation of ICP-OES method to determine Sb in drinking water

Parameter	Unit	Value
Liniarity, r	-	0,9992
Detection limit, LoD	µg L^{-1}	1,14
Quantification limit, LoQ	µg L^{-1}	3,42
Repeatability, s_r	µg L^{-1}	0,55

Relativ standard deviation, RSD	%	4,98
Accuracy, as difference, δ	μg L^{-1}	0,31
Accuracy, as degree of recovery, R	%	103
Extended uncertainty, U (k=2, P=95%)	μg L^{-1}	1,7

Conclusions

The developed and validated method for the determination of Sb in drinking water (tap water) provided the following performance parameters: for linearity, the value of the correlation coefficient $r \geq 0.9992$, the limit of detection 1.14 μg L^{-1} and the limit of quantification 3.42 μg L^{-1}. Repeatability value obtained was 0.55 μg L^{-1}, the accuracy value also was of + 0.31 μg L^{-1} and the recovery value obtain was 103%. The extended uncertainty value was 1.7 μg L^{-1} with a confidence level of 95% (k=2). In the absence of interlaboratory collaborative results for determining method performance, the composed uncertainty provides a reasonable estimation of the reproducibility.

4. 2. METHOD FOR SB DETERMINATION FROM BOTTLED NATURAL MINERAL WATERS

4.2.3 Validation of the method for Sb determination from natural mineral water by calibration curve method

The relevant performance parameters of the developed method were: linearity, precision (repeatability), accuracy, measurement uncertainty, limits of detection (*LoD*) and quantification (*LoQ*). This study is the subject of a published article [214].

Liniarity

Linearity was evaluated based on the regression function of calibration by using five standard solutions prepared in a range of concentrations between 2 - 20 μg L^{-1}. The equation of the calibration curve is presented is shown in Figure 14. The linearity, fulfills the acceptance criterion (Table 20), based on a correlation coefficient, r=0.9992.

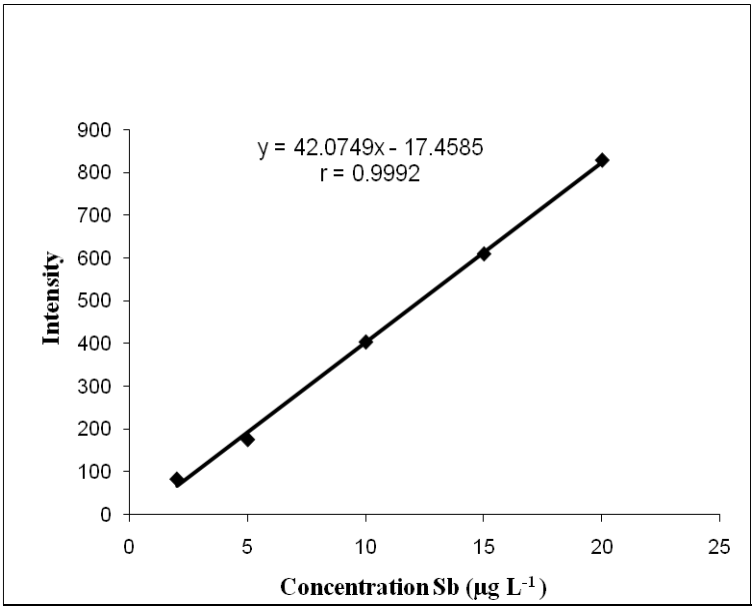

Figure. 14. Calibration curve for the concentration range 2 µg L^{-1} to 20 µg L^{-1} Sb

*Limits of Detection **(LoD)** and Quantification **(LoQ)***

For determination of the limit of detection (*LoD*) and limit of quantification (*LoQ*), ten standard solutions were measured with the smallest concentration on the calibration curve, i.e. 2 µg L^{-1}. The standard deviation of the determinations set with an average content of 2.04 µg L^{-1} was 0.22 µg L^{-1}. The limits of detection (*LoD)* and quantification (*LoQ*) were calculated using formula (Eqs.13-14) obtaining the following results: 0.67 µg L^{-1} and respectively 2.01 µg L^{-1}.

The results for *LoD* and *LoQ* fulfill the acceptance criteria presented in Table 19.

Precision (Repeatability)

The repeatability of the method has been determined by measuring ten samples of the same concentration, closed to the maximum admissible one in repeatability conditions. The value of the standard deviation (s_r) was obtained at an average content of 4.10 µg L^{-1} is 0.25 µg L^{-1}, thus acceptance criteria being fulfilled. The obtained RSD was 6.21 %.

Accuracy

The accuracy of the method was determined in two different ways presented below:

• as difference (δ), between the average content of ten measurements of 10 µg L^{-1} standard solutions and theoretical antimony content of reference material (10 µg L^{-1} Sb); the obtained result, δ = 0.16 µg L^{-1}, fulfills the acceptance criterion presented in Table19.

• as degree of recovery, based on the method of standard additions, applied to three types of mineral water consisting in adding different volumes of 100 mg L^{-1} Quality Control Standard 21 standard solution (Perkin Elmer, USA), in the analyzed samples; thus the mineral water samples were fortified with a standard solution at three levels of concentration (Table 17) and analyzed in triplicate.

Accuracy (% the recovery degree) was measured as the difference between the concentration of the spiked and unspiked sample, compared to the concentration of the analyte added to the spiked sample. The accepted values for the recovery degree depending on the analyte concentration must be within the domain 40 % ≤R % ≤120 % [210]. The results of the study are presented in Table 19. The obtained recovery degree values stand in the 95 % - 109 %, and fulfilled the required criteria for all levels of the tested concentrations.

Table 17. The obtain results of recovery degree

Sample	Sb			R (%)
	$C_{measured}$ (µg L^{-1})	$C_{calculated}$ (µg L^{-1})	R (%)	Average recovery degree on sample
Sample 1	0.344	-	-	-
Sample 1 + 2 µg L^{-1}	2.39	2.05	102	106
Sample 1+ 5 µg L^{-1}	5.67	5.33	107	
Sample 1+ 10 µg L^{-1}	11.2	10.9	109	
Sample 2	0.475	-	-	-
Sample 2 + 2 µg L^{-1}	2.35	1.95	97.5	97.1
Sample 2+ 5 µg L^{-1}	5.24	4.77	95.4	
Sample 2 + 10 µg L^{-1}	10.3	9.83	98.3	
Sample 3	0.613	-	-	-
Sample 3 + 2 µg L^{-1}	2.73	2.12	106	101
Sample 3+ 4 µg L^{-1}	4.48	3.87	96.8	
Sample 3+ 6 µg L^{-1}	6.66	6.05	101	

Average recovery degree of the method was R = 102%.

The statistical test:

$$t = (100 - \overline{R}) / s_{\overline{R}} \leq t_c \qquad (19)$$

where: $\overline{R}$ - average recovery, % ;

$s_{\overline{R}}$ - standard deviation of recovery;

t_c - critical *t* value;

Calculated *t* value, applied to the recovery degrees does not emphasize the existence of any systematic errors due to matrix or method.

The values obtained by using the calculated *t*-test (Ec. 19) are between 0.275 and 3.500 and do

not exceed the critical value, t_c = 4.303, n = 2 and a confidence level of 95 % [213].

Quantification of uncertainty

Uncertainty sources that significantly affect the concentration are presented in Table 18.

Table 18. The budget of uncertainty of the method of determining Sb in mineral water.

Component u(x)	Source	Value	Unit	Standard uncertainty	Relative standard deviation, RSD %
u (δ)	Accuracy	10,16	µg L^{-1}	0,16	1,09
u (Rep)	Repeatability	4,10	µg L^{-1}	0,25	6,09
u (c)	Calibration curve fitting	4,10	µg L^{-1}	0,43	10,5
u (*P*)	Standard purity	1	-	0,0029	0,29

The uncertainty of determination of concentration based on calibration curve, u*(c)* is determined using formulae 15-17 [213].

The combined uncertainty u_c, calculated based on the uncertainties associated with each component, according to the rule of propagation of uncertainty [213], is:

$$u_c = c \times \sqrt{\left(\frac{u(\delta)}{\delta}\right)^2 + \left(\frac{u(\mathrm{Re}\, p)}{\mathrm{Re}\, p}\right)^2 + \left(\frac{u(P)}{P}\right)^2 + \left(\frac{u(c)}{c}\right)^2} \qquad (20)$$

The composed uncertainty (u_c) based on (Ec. 20) for the determination method of Sb with a content level of 4.10 µg L^{-1}, expressed as standards deviation, is, este u_c =0,5µg L^{-1}. In the absence of an inter-laboratory study for determination of the performance of the method, the composed uncertainty gives a reasonable estimation of reproducibility.

For a 4.10 µg L^{-1} average concentration and a cover factor of k = 2, corresponding to a confidence level of 95 %, the extended uncertainty is 1.0 µg L^{-1}.

Table 19. Performance parameters of the method for Sb determination from natural mineral water by calibration curve method (CCM) and acceptance criteria

Parameter	Value	Unit	Acceptance criteria
Linearity, r	0,9992	-	≥ 0,997
Detection limit, LoD	0,67	µg L^{-1}	1,25
Quantification limit, LoQ	2,01	µg L^{-1}	3,75
Repeatability, s_r	0,25	µg L^{-1}	1,25
Accuracy, as difference, δ	0,16	µg L^{-1}	1,25

Accuracy, as degree of recovery, R	102	%	40% ÷ 120%
Incertitudine extinsă,U (k = 2, P = 95 %)	1,0	µg L^{-1}	2,0

The results from the "in house" validation study (Table 19) show that all the performance criteria are fulfilled.

4.2.4. Analysis of mineral water samples by using the method of standard additions

In order to eliminate the interferences due to the matrix, the samples were analyzed by the method of standard additions (SAM). Comparative data are presented in Table 21.

Table 21. Comparative results of Sb determination by CCM and SAM methods in mineral waters from Romania

Mineral water samples	Sb (µg L^{-1})		$u_{c,}$ (µg L^{-1})	Linearity, r		LoD, (µg L^{-1})		LoQ, (µg L^{-1})	
	CCM	SAM	SAM	CCM	SAM	CCM	SAM	CCM	SAM
Sample 1	0,344*	0,254	0,053	0,9992	0,9999	0,67	0,157	2,01	0,473
Sample 2	0,475*	0,422	0,065	0,9992	0,9999	0,67	0,195	2,01	0,587
Sample 3	0,613*	0,641	0,125	0,9992	0,9990	0,67	0,375	2,01	1,13

* the marked values are below the detection limit (LoD) of the calibration curve method (CCM)

It is found that all analyzed waters comply with requirement EU Directive 2009/54/EC, presenting values of the concentration below the limit of detection of the method. The tested mineral waters fulfill the acceptability condition for the maximum admissible concentration of antimony of 5 µg L^{-1}, required by EU Directive 2009/54/EC and Government Decision no. 1020/2005, and it is smaller than the quantification limit of the method.

Standard Additions Method (SAM) offers some great advantages: it overcomes matrix interferences [225] and it decreases the limit of detection from 0.67 to 0.16 µg L^{-1}. This decrease is due to the fact that standard additions are correlated with the measured Sb concentrations in the studied matrices, decreasing the component of the uncertainty through covariance.

Conclusions

Also, an accurate analytical method for the determination of Sb in natural mineral water with direct analysis of mineral water samples was developed in this study. It represents a simple, cheap and fast measurement, characterized by high recovery at low concentration of Sb determined from carbonated mineral water, by ICP-OES technique. Over the studied concentration range, the calibration curve slope, expressed through correlation coefficient r = 0.9992, limits of detection *LoD* = 0.67 µg L^{-1} and quantification *LoQ* = 2.01 µg L^{-1}, a value of 0.25 µg L^{-1} for standard deviation of repeatability, accuracy of 0.16 µg L^{-1} satisfy the acceptance criteria. The concentration of Sb in the analyzed mineral waters is below the *LoD* of the CCM developed method. Thus, Sb from the same mineral waters has been analyzed by standard additions method (SAM). The correlation coefficients of the calibration curves obtained by the method of standard additions ranged between r = 0.9990 and r = 0.9999, SAM offering some great advantages regarding the matrix interferences and decreasing the limit of detection from 0.67 to 0.16 µg L^{-1}.

4.3. The method for Sb determination from PET by ICP-OES

The scope of the present work is to develop a simple, cheap and quick method for Sb determination from PET until 500 mg Kg^{-1} range, using an original digestion method which presents superior performances as compared to the methods specified in the literature, coupled with the ICP-OES technique. This study is the subject of a published article [226].

PET samples

Five PET samples from different drinks such as still (non-carbonated) water, sparkling (carbonated) water, carbonated beverages, beer from different brands, were purchased from a supermarket. Table 22 describes the PET bottle samples.

Table 22. Presentation of PET bottle samples

PET bottle sample	Beverage	Colour of the PET
1	Sparkling water	Transparent
2	Carbonated beverages	Green
3	Still water	Light blue
4	Still water	Transparent

PET digestion method

The PET samples cans are cut in pieces of 1.0 x 1.0 mm, using a ceramic knife and washed with ultrapure water. The samples of 0.1 grams are weighed with analytical precision of 0.1 mg. The sample is then quantitatively transferred in the digestion vessel made of PTFE - TFM and 8 mL HNO_3 (65 %) are added. The two stages of the microwave digestion were: first stage performed at 160°C for 20 minutes, while the second stage at 190°C for 25 minutes, both at 800W power. The digested samples are then diluted with ultrapure water to 100 mL in a flask, obtaining a clear solution.

Experimental method for Sb analysis using ICP-OES

The operation parameters for ICP-OES equipment are presented in cap. 4.1.2. The standard solutions of 10; 100; 200; 300; 400 and 500 µg L^{-1} used for development of the calibration curve, were obtained by diluting the stock solution of 100 mg L^{-1}, Quality Control Standard 21.

4.3.2. Method optimization. Digestion of Sb from PET

The development and optimization of the method consisted of the variation of main working parameters, i.e. type and concentration of reagent (HNO_3, H_2O_2, H_2SO_4), temperature and digestion time. In the case of PET digestion with HNO_3 (65 %) and H_2O_2 (35 %), an opaque solution was obtained, fact reported also by Ying-Ying et al. [231]. In ICP-OES analysis, it is highly recommended a clear solution, ensuring thus a complete mineralization and not retaining the analyzed compound in solid particles. This inconvenient can be removed by adding sulfuric acid (98 %) while continuing the digestion on sand bath until clear solution. On the other hand the caveat is a larger time and increased number of necessary operations.

Digestion with HNO_3 (65 %) and H_2SO_4 (98 %) has many caveats: the reaction is highly exothermic with risk of damaging of reaction vessels by over-heating. The acid mixture is also foaming with the risk of losing parts of sample. The use of sulfuric acid reduces lifetime of vessels and gaskets because of its corrosive properties [234]. On the other hand, sulfuric acid can affect background emissions observed in ICP-OES, causing interferences in analysis. From this point of view, nitric acid (65 %) is recommended for sample preparation [111].

The performance parameters of the developed method were: linearity, precision (repeatability), accuracy, the recovery degree, uncertainty, limits of detection (LoD) and quantification (LoQ). The acceptance precision criterion is calculated based on Horwitz equation [235]:

$$RSD \leq 0{,}6 \times 2^{(1-0{,}5 \lg C)} \quad (21)$$

where: C is the sample concentration expressed as mass fraction

The acceptance criterion for measurement uncertainty is U:

$$U \leq 2 \times s_R \quad (22)$$

where:

s_R is relative standard deviation and is calculated with formula:

$$s_R = \frac{RSD \times C}{100} \quad (23)$$

where, RSD is calculated using Horwitz equation (Ec. 21).

4.3.3. Validation of the method for Sb determination from PET

The key performance parameters for other methods in the literature and results from the "in house" validation study and acceptance criteria for this method presented in Table 26 show that all the performance criteria are fulfilled.

Table 26. Key performance parameters for other methods in the literature in comparison with working method and acceptance criteria.

Performance parameter	Reported value	Reference	Performance parameters of our method	Acceptance criterion for proposed method	Refe-rence
Linearity, r	R = 0,998	[206]	0,9999	r ≥0,997	[210]
Precision (repeatability)	RSD = 0,7 – 2,0 %;	[232]	0,49 %	RSD < 4,6 %	[235]
Accuracy (recovery degree, R)	97-98 % 102 %	[206] [232]	89,7 %	80 % ≤ R % ≤ 110 %	[210]
Measurement uncertainty, U	2,75 – 50,0 mg Kg^{-1}	[227],[224] [230], [231],[232] [222,233]	8,4 mg Kg^{-1}	U≤ 36 mg Kg^{-1}	[235]
Limit of Detection, LoD Limit of Quantification, LoQ	LoD: 0,3 µg L^{-1}; LoQ: 1,0 µg L^{-1}; LoD: 1,8 mg Kg^{-1}; LoQ: 6,0 mg Kg^{-1};	[230] [206]	LoD:10,2 mg Kg^{-1} LoQ: 20,4 mg Kg^{-1}	LoD≤25 mg g^{-1} LoQ≤50 mg Kg^{-1}	[210]

Conclusions

The study presents a simple, cheap and quick way of antimony determination from PET in the range of 10 - 500 mg Kg^{-1}, based on an original digestion method coupled with ICP-OES measurement technique. The digestion method, developed and optimized for this study, uses only one digestion reagent (HNO_3), in comparison with other methods presented in the literature and shorter digestion time, too. The reagent is friendly to the measurement equipment, ensures a reduced digestion time (45 min.), thus having small energy consumption (0.15KWh/sample) and requesting standard digestion equipment.

On the studied concentration range, the calibration curve slope, expressed through correlation coefficient r = 0.9999, standard deviation of repeatability of 1.27 mg Kg^{-1}, RSD = 0.49 %, accuracy determined by recovery degree ranges between 85 % and 96 % satisfy the demands of chemists for these parameters, being comparable with literature data. The value of extended uncertainty is 8.4 mg Kg^{-1} with a confidence level of 95 % (k=2), obtained for Sb content of 260 mg Kg^{-1}.

The applicability domain of the method can be extended to higher-contents with the same digestion method and corresponding modification of calibration curve. The validated method can be applied for determination of antimony content from PET.

CONCLUSIONS

The experimental studies presented in this chapter aimed to develop and validate several methods of Sb determination in drinking water as well as to develop and optimize a method of determination of Sb in PET.

In conclusion, the developed methods can be applied to determine the Sb content for drinking water quality control, as regulated by Law 458/2002 with subsequent additions [175] and EU Directive 1998/83/EC [183], as well as natural minerals waters according to Government Decision no. 1020/2005 and EU Directive 2009/54/EC, but also in research studies on the migration of Sb from PET into various beverages.

CHAPTER 5

SORBTION OF INORGANIC COMPOUNDS WITH HARMFUL EFFECTS ON HUMAN ORGANISM

5.1. Adsorption of Sb (III) on oxidized exfoliated graphite nanoplatelets (ox-xGnP).

The purpose of this study was to evaluate the potential of ox-xGnP as an adsorbent for Sb (III). This is the novelty because it is for the first time, based on our knowledge, when oxidized exfoliated nanoplatelets graphite (ox-xGnP) are applied as sorbents for Sb (III). In order to accomplish the goal, the objectives were to study the following influences: influence pH of solutions, influence of ox-xGnP, influence of contact time, influence of Sb (III) initial concentration and influence of temperature on the sorption process. The kinetics and the adsorption isotherms of the process were studied to achieve the best kinetic model and the best isotherm equation, respectively. In addition, the thermodynamic parameters were studied.There is also a series of applications of Sb (III) adsorption on ox-xGnP from different types of water and a mechanism of adsorption of Sb (III) on ox-xGnP that is proposed. The research presented in this chapter is the subject of a published article [236].

Few studies on the adsorption of Sb (III) on carbon nanomaterials are found in the literature [3,112,119], so the choice of the adsorbent used in this study is justified by the fact that exfoliated nanoplatelets graphite (xGnP) exhibit good stability as well as adsorption efficient and fast. The adsorption capacity of this new nanostructured adsorbent material is high [237]. In addition, xGnP could be a suitable substituent for carbon nanotubes and fullerenes because of their low cost [89].

Based on previous studies of sorbent types presented in a published article [238], it was found that physico-chemical parameters strongly influence the dispersion of carbon nanomaterials, exfoliated nanoplatelets graphite (xGnP) compared to coal dispersions (AC) in tetrahydrofuran (THF), providing new information about the structure and interactions of carbon nanostructures in organic [239].

5.2.2. *Synthesis of ox-xGnP and characterization methods*

The xGnP (black powder) was functionalized by chemical oxidation to obtain ox-xGnP, according to the method presented in references [216,243]. For the characterization of ox-xGnP before and after adsorption, the following methods and equipment were used:

Thermogravimetric analysis (TGA) was performed using the Mettler Toledo (Columbus, OH, USA) TGA/SDTA 851 apparatus in nitrogen atmosphere with alumina crucibles in the temperature range of 50–550 °C and a heating rate of 1 °C min^{-1}. The Brunauer–Emmet–Teller (BET) specific surface area of the ox-xGnP was characterized by nitrogen adsorption using a Quantachrome NOVA 2200e instrument (Boynton Beach, FL, USA). Nitrogen adsorption–desorption isotherm was measured at the temperature of liquid nitrogen (77 K). Prior to measurements, the samples were degassed at 60 °C in vacuum for 4 h. The specific surface area was calculated according to the BET equation. The total pore volume was estimated from the amount of gas adsorbed at a relative pressure $p/p_o = 0.99$. The classical Barrett–Joyner–Halenda (BJH) model applied to the adsorption branch of the isotherm was used to determine mesopores' surface area, mesopores' volume, and mesopores' size distribution, respectively [109]. Zeta potential was obtained from the electrophoretic mobility by using the Smoluchowsky model. The electrokinetic measurements were carried out with the Zetasizer Nano ZS, Malvern Instruments Ltd., UK. The ζ-potential can be used as an indicator of the electrostatic stabilization of particles. The electrokinetic measurements were performed on ox-xGnP at different pH values. Fourier transform infrared spectroscopy (FT-IR): spectra were recorded on a Spectrum GX spectrometer Perkin Elmer (Waltham, MA, USA) in transmittance, in KBr pellets, by accumulation of 32 spectra, with a resolution of 4 cm^{-1}. Scanning Electron microscopy (SEM): the images were obtained with a FEI QUANTA 200 (FEI Company, Hillsboro, OR, USA) equipment operating at a 30 kV electron acceleration voltage, high vacuum, direct on uncovered samples. The microscope Tecnai™ G2 F20 TWIN Cryo-TEM, 2015 (FEI Company, Eindhoven, The Netherlands) was used to perform classical TEM (BF-TEM) and scanning transmission electron microscopy (STEM) analyses on final materials. The powders were well dispersed in ultrapure water by ultrasonic treatment of the samples. EDX (single point) was also used to determine the presence of different elements. A small drop of well-dispersed sample was placed on the copper grid and visualized by TEM.

5.2.3. Description of the adsorption experiments

A stock solution of 100 mg L^{-1} Sb (III) used in the adsorption experiments was prepared by dissolving 0.137 g of potassium antimony tartrate in a 500 mL volumetric flask with ultrapure water. From the stock solution, work solutions with the concentrations of 0.1 mg L^{-1}, 0.3 mg L^{-1}, 0.5 mg L^{-1}, 0.7 mg L^{-1}, and 1.0 mg L^{-1} were prepared by dilution. The pH of the working solutions was adjusted by adding small amounts of 0.1 or 0.01 M KOH solution and 0.1 M HCl. For the study of the adsorption kinetics, solutions were prepared by adding 100 mL of solution adjusted to pH = 4.0, 5.0, 7.0, 9.0, and 11.0 over 1.0 mg of ox-xGnP. After ultrasonic treatment

of ox-xGnP for 30 min, adequate volumes of Sb (III) stock solution to obtain the concentrations of 0.1 mg L^{-1}, 0.3 mg L^{-1}, 0.5 mg L^{-1}, 0.7 mg L^{-1}, and 1.0 mg L^{-1} were added.

The dispersion of -ox-xGnP was performed using an Ultrasonic Processor VCX 750 (Newtown, CT, USA) with a frequency of 20 kHz and an ultrasonic bath Elma P-30H Ultrasonic (Landsberger, Berlin) operated at a frequency of 37 Hz at 20 °C, 25 °C, and 30 °C. After completion of the adsorption experiments, the suspensions were filtered into 2.0 mL glass vials using a 0.2 µm RC filter attached to a syringe, and the concentration of Sb was analyzed by the ICP–OES Optima 2100 DV System (Perkin Elmer, Waltham, MA, USA) with dual optics view. All experimental data were obtained in triplicate, and the relative standard deviations were <5%. The models were calculated on the basis of the average of the values obtained for each point.

The adsorption capacity q_t (mg g^{-1}) was calculated by Equation:

$$q_t = \frac{(C_0 - C_x)}{m} \times V \qquad (28)$$

where C_0 (mg L^{-1}) and C_x (mg L^{-1}) are the initial concentration of Sb (III) in solution and the concentration at time *t*, respectively; *V* (L) is the volume of solution; *m* (g) is the mass of ox-xGnP.

In real water samples the sorption experiments were carried out according to the method described in chapter 5.2.3.

5.3. Characterization of ox-xGnP

The TGA curve of the ox-xGnP is shown in Figure 21. From the obtained thermogram, a very small rise of the mass (%) of about 1% can be observed between 50 and 130 °C, which might be be explained by the adsorption of N_2 on the xGnP surface, but the major change observed from the thermogram is a decrease of the mass loss of 4.1% between 130 and 550 °C, which can be attributed to the release of CO and CO_2, according to the literature [244].

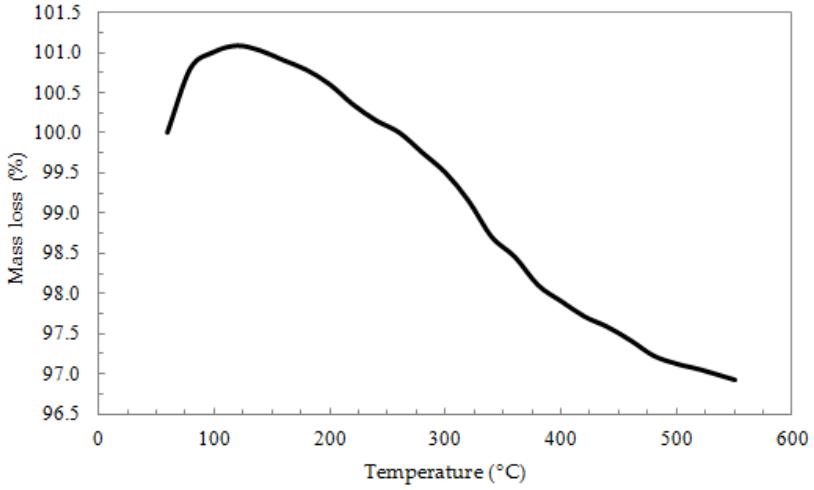

Figure 21. TGA of oxidized exfoliated graphite nanoplatelets (ox-xGnP).

The following results from the N_2 physisorption analysis of ox-xGnP were obtained: mesopores' surface area = 205 m^2 g^{-1}, mesopores' volume = 0.33 cc g^{-1}, and mesopores' diameter = 3.9 nm, respectively.

Figure 2 compares the FT-IR spectrum of ox-xGnP with that of ox-xGnP on which Sb (III) from antimony potassium tartrate was adsorbed, (ox-xGnP+Sb). In this study, the spectral zone from 1800 cm^{-1} to 1000 cm^{-1} was analyzed.

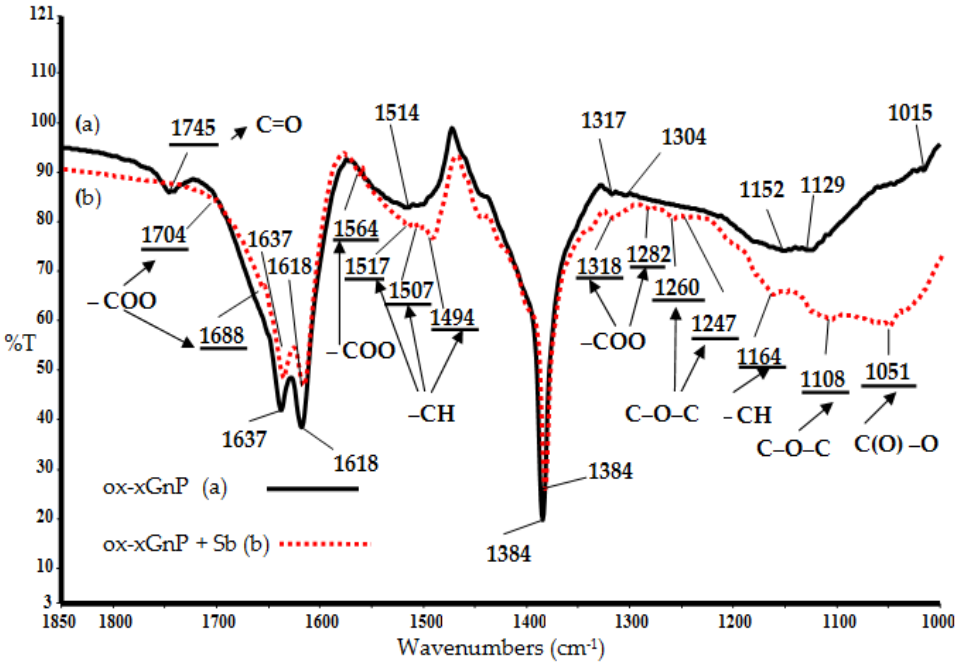

Figure 22. FT-IR spectra (a) ox-xGnP before adsorption of Sb (III); (b) ox-xGnP after adsorption of Sb (III) (ox-xGnP+Sb)

The occurrence of Sb (III) adsorption was highlighted by the disappearance of the 1745 cm^{-1} vibration band, specific to the C=O group, from the oxidized graphite and the appearance of vibration bands for –COO at 1704 cm^{-1}, 1688 cm^{-1}, 1564 cm^{-1}, 1318 cm^{-1}, and 1282 cm^{-1}. The vibration bands specific to the C–O–C group at 1260 cm^{-1}, 1247 cm^{-1}, 1108 cm^{-1} and that specific to the C(O)–O group at 1051 cm^{-1} [246] were observed both before and after adsorption. Additionally, the absorption bands at 1517 cm^{-1}, 1507 cm^{-1}, 1494 cm^{-1}, and 1164 cm^{-1}, specific for the –CH groups, were observed after the adsorption process [247-250].

The morphological study of the oxidized nanomaterials ox-xGnP and ox-xGnP+Sb was performed by scanning electron microscopy. The SEM images of secondary electrons for ox-xGnP with a magnification of 10,000× and 15,000× are presented in Figure 23 a,c, respectively. A morphology of extremely thin films was observed, with a slight tendency of crowding and marginal twisting and the presence of bright, rounded, and polyhedral particles of Sb with

relatively uniform layout on the samples after the sorption of Sb (Figure 23b,d). The SEM images confirmed the adsorption of Sb on ox-xGnP.

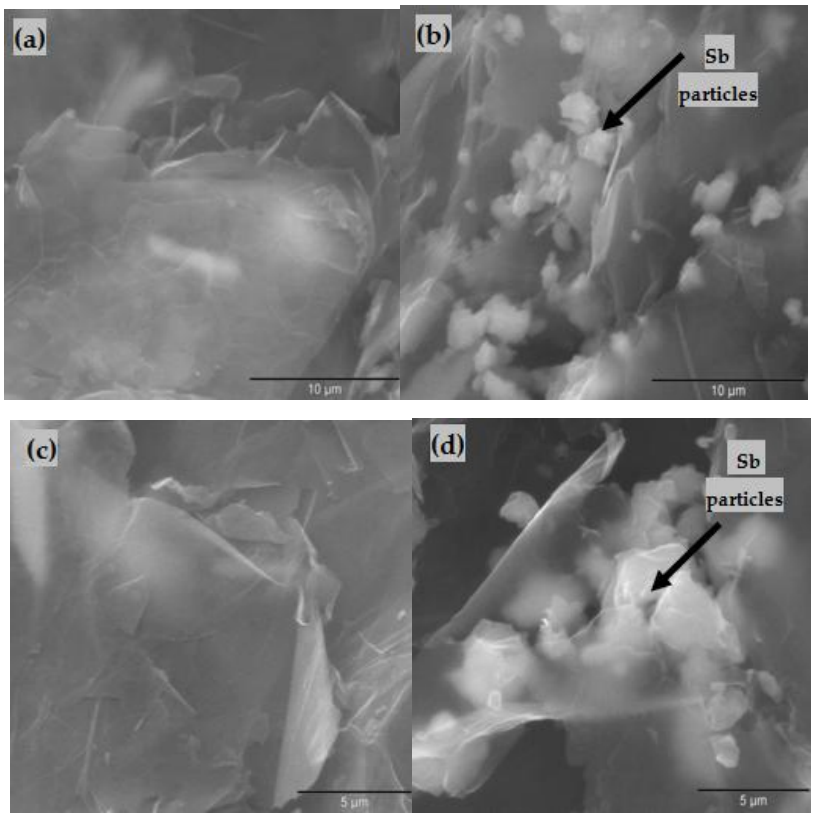

Figure 23. SEM images (**a**,**c**) ox-xGnP before adsorption of Sb at magnifications of 10,000× and 15,000×, respectively; (**b**,**d**) ox-xGnP after adsorption of Sb at magnifications of 10,000× and 15,000×, respectively

In Figure 24a, a TEM image of ox-GnP before adsorption of Sb is shown, whereas in Figure 24b, a STEM image of ox-GnP after adsorption of Sb is shown. Both micrographs show a mostly agglomerated structure, the first one having a wrinkled paper morphology due to the initial xGnP morphology [100]. Imagimea The STEM image presents Sb particles having a non-regular shape (as in SEM images), with sizes between 50 and 200 nm. The ox-xGnP sample did not present the wrinkled paper morphology. In Figure 4c, EDX indicated the presence of small quantities of Sb.

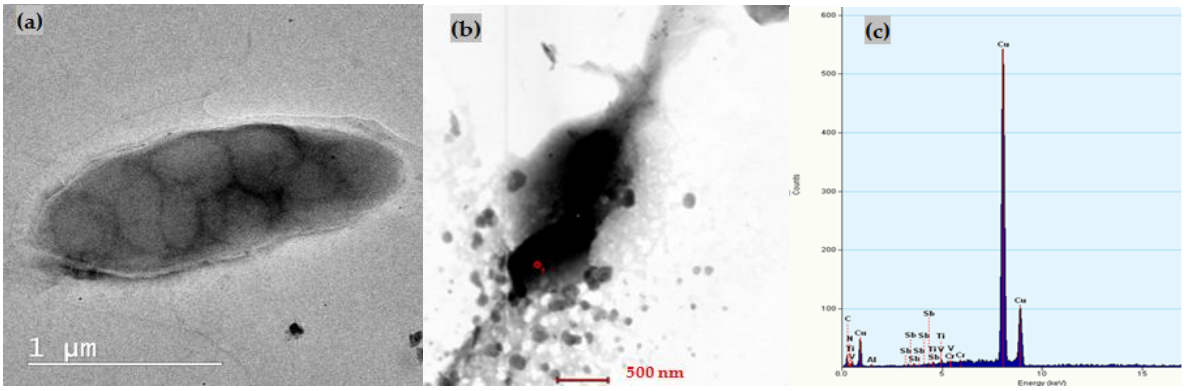

Figure 24. (**a**) TEM micrograph of ox-xGnP before adsorption of Sb; (**b**) STEM image of ox-xGnP after adsorption of Sb; (**c**) EDX analysis of ox-xGnP after adsorption of Sb

5.4. Adsorption Study. Effects of the Adsorption Parameters

In order to optimize the adsorption of Sb (III) on ox-xGnP from aqueous solution, the effects of the following parameters were investigated: the pH of the sorption solutions, the amount of ox-xGnP, the contact time and the temperature at which the adsorption process took place, and the initial concentration of Sb (III).

5.4.1. The Effect of pH on the adsorption capacity of Sb (III) from aqueous solutions studied in the pH range of 4.0–11.0.

In the range of pH 5.0–9.0, a significant increase in the adsorption capacity of Sb (III) on the ox-xGnP surface, from 7.40 to 16.0 mg g^{-1}, was observed; then, the adsorption decreased, reaching a value of 9.60 mg g^{-1} at pH 11.0, as shown in Figure 25. The influence of the solution pH on the adsorption capacity is a complex phenomenon influenced by both the metal ion species in the solution and the modifications of the functional groups on the surface of the adsorbent material.

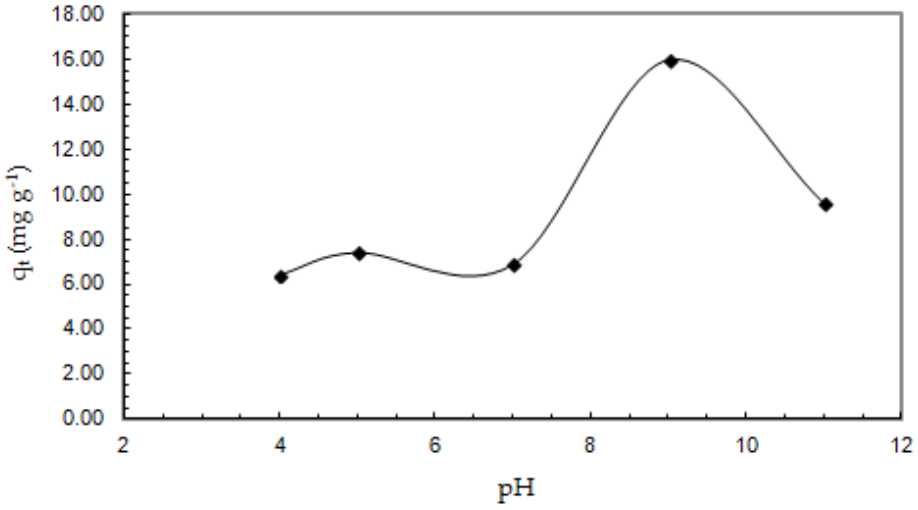

Figure 25. The effect of solution pH on the adsorption capacity of Sb (III) onto ox-xGnP (0.7 mg L^{-1} Sb (III), 1.0 mg ox-xGnP/100 mL solutions, T = 20 °C and contact time 30 min)

The negative charge of the surface ox-xGnP confirmed by Zeta's potential analysis (Figura 26) provided favorable interactions for the adsorption of cationic species. By increasing the pH, the values of ζ-potential varied from −13.7 mV (pH = 4.0) to −63.4 mV (pH = 9.0). The higher the value of pH, the more negative the net charge of ox-xGnP; at pH 9.0, the highest colloidal stability due to the electrostatic repulsion between particles was observed.

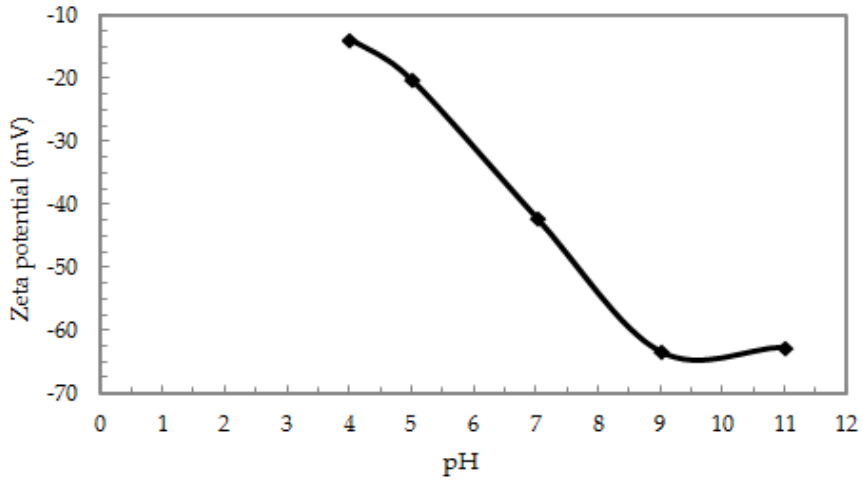

Figura 26. Zeta potential curve of ox-xGnP suspension versus solution pH

In the pH range between 4.0 and 10.0, the species of Sb, (III) according to the literature are $[HSbO_2]$ and $Sb(OH)_3$ in aqueous solution. At pH values > 10.0 the presence of the species $Sb(OH)_4^-$ and $[SbO_2]^-$ was previously mentioned [253,254]. The experiments were done at pH 7.0, in view of further applications of these results for Sb (III) removal from drinking water, the common pH range of which is between 6.0 and 8.0.

5.4.2. Effect of the amount of ox-xGnP on the adsorption process

To evaluate the influence of ox-xGnP amount on adsorption, the sorption experiments were performed at pH = 7.0, T = 293 K, Sb concentrations of 0.3 mg L^{-1} and 0.7 mg L^{-1}, and amounts of ox-xGnP 1.0 and 2.0 mg. The data presented in Table 28 show a lower adsorption capacity with increasing adsorbent amounts. Therefore, in the following experiments, 1.0 mg of ox-xGnP was used.

Tabel 28. Effect of sorbent amount on the sorption capacity.

Amount of ox-xGnP (mg)	Concentration of Sb (III) (mg L^{-1})	qe (mg g^{-1})
1,0	0,3	3,60
1,0	0,7	6,86
2,0	0,3	2,85
2,0	0,7	5,10

5.4.3. Effect of the initial concentration of Sb (III) on the adsorption process

Figure 27 shows the variation of the adsorption capacity with the contact time for an amount of ox-xGnP corresponding to 1.0 mg and initial concentrations of Sb of 0.1, 0.3, 0.5, and 1.0 mg L^{-1}. The adsorption capacity increased by increasing the initial concentration of Sb (III). Stationary (steady) values of adsorption capacity were reached in all experiments after about 25 min.

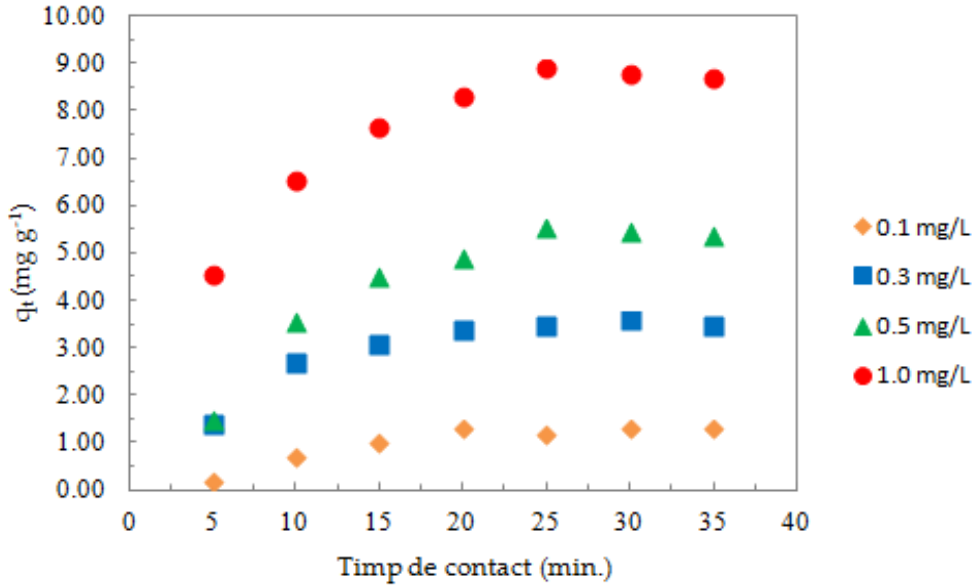

Figura 27. The effect of the initial Sb (III) concentration on its sorption on ox-xGnP (pH 7.0, 1.0 mg of ox-xGnP/100 mL solution, T = 20 °C)

5.4.4. Effect of Contact Time and Temperature on the Adsorption Process

The effect of contact time and temperature on the adsorption process was studied for systems containing 1.0 mg of ox-xGnP in solutions of Sb (III) with initial concentration of 1.0 mg L^{-1}, at pH 7.0 and Temperatures of 20 °C, 25 °C, and 30 °C, as shown in Figure 28.

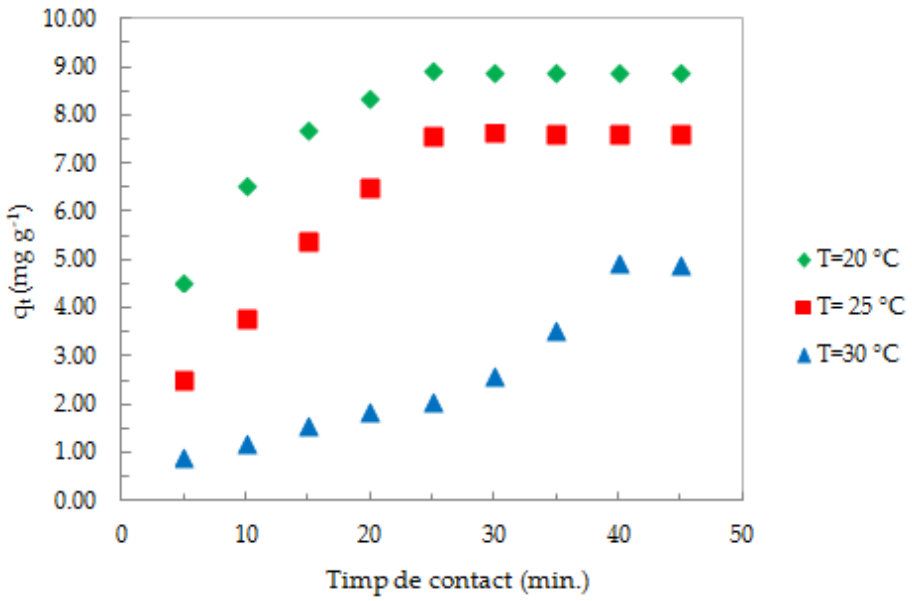

Figura 28. Effect of contact time and temperature on the adsorption of Sb (III) onto ox-xGnP (pH = 7.0, 1.0 mg L^{-1} Sb (III), 1.0 mg of ox-xGnP/100 mL solution)

An initial increase of the adsorption capacity (qt) of Sb (III) was observed during the first 20 min, after which it remained constant. By increasing the temperature, the values of the adsorption capacity decreased. The time required to reach the equilibrium in the temperature range 20–30 °C varied between 25 and 40 min.

Considering the parameters variation, the optimal working conditions were the following: pH = 7.0, 1.0 mg ox-xGnP/100 mL solution, T = 293 K, 1.0 mg L^{-1} Sb (III), 25 min contact time.

5.5. Adsorption Kinetics Study

The experimental data obtained in this study were evaluated on the basis of three kinetic models, namely, the pseudo-first-order kinetic model, the pseudo-second-order kinetic model, and the intra-particle diffusion, to investigate the kinetics of the adsorption mechanism.

The equation of the pseudo-first-order kinetic model, given by Lagergren [266] is written as follows:

$$\ln(q_e - q_t) = \ln q_e - k_1 t \qquad (29)$$

where, q_t is the amount of Sb (III) adsorbed on ox-xGnP at time t (mg g^{-1}), q_e is the amount of Sb (III) adsorbed on ox-xGnP at equilibrium (mg g^{-1}), k_1 is the rate constant of the pseudo-first-order equation (min^{-1}), and t is the contact time (min). The rate constant k_1 was obtained from the representation ln (qe − qt) versus t.

The data obtained for the adsorption of Sb (III) on ox-xGnP were also analyzed by the pseudo-second order of kinetics, given by the following equation [267,268]:

$$\frac{t}{q_t} = \frac{1}{k_2 q_e^2} + \frac{t}{q_e} \qquad (30)$$

where, q_t is the amount of Sb (III) adsorbed on ox-xGnP at time t (mg g^{-1}), q_e is the amount of Sb (III) adsorbed on ox-xGnP at equilibrium (mg g^{-1}), k_2 is the rate constant of the pseudo-second-order equation (g $mg^{-1}min^{-1}$), and t is the contact time (min). The rate constant k_2 was obtained from the dependence t/qt versus t.

The intra-particle diffusion model [269] is given by the following equation:

$$q_t = k_{i_d} t^{1/2} + C \qquad (31)$$

where, q_t is the amount of Sb (III) adsorbed on ox-xGnP at time t (mg g^{-1}), k_{id} is the intra-particle diffusion constant (mg $g^{-1}min^{-1/2}$), t is the contact time ($min^{1/2}$), and C (mg g^{-1}) is a constant, proportional to the thickness of the boundary layer. The constant k_i is obtained from the representation q_t versus $t^{1/2}$. The criterion for assessing the applicability of the three kinetic models was the determination coefficient presented in Table 29.

The highest value of R^2 was obtained with the pseudo-first kinetic model. Moreover, the value of the adsorption capacity obtained experimentally at equilibrium was in accordance with the value of adsorption capacity calculated by the pseudo-first kinetic model (Table 29), which indicated that the adsorption process of Sb (III) on ox-xGnP fit better with this model.

Tabel 29. Parameters obtained for different kinetic models of the adsorption of Sb (III) on ox-xGnP, at T = 293 K

$q_{e\ exp.}$ (mg g^{-1})	Pseudo-First-Order Kinetic Model			Pseudo-Second-Order Kinetic Model			Intra-Particle Diffusion Model		
	Model parameters		Performance parameter	Parametrii modelului		Performance parameter	Model parameters		Performance parameter
	$q_{e\ cal.}$ (mg g^{-1})	k_1 (min^{-1})	R^2	$q_{e\ cal.}$ (mg g^{-1})	k_2 (g mg^{-1} min^{-1})	R^2	k_{id} (mg g^{-1} $min^{-1/2}$)	C (mg g^{-1})	R^2
8,91	8,10	0,129	0,999	11,3	199	0,998	1,64	1,17	0,978

5.6. Study of adsorption isotherms

The adsorption isotherms describe how the adsorbed Sb (III) interacts with the ox-xGnP, providing information about the nature of the interactions that occur in the process. To describe these processes, the Langmuir and Freundlich models, the equations of which are presented below, were used in this study.

The Langmuir model is a model based on monolayer adsorption and surface homogeneity, the equation (1) [151]. Another important parameter calculated from the Langmuir isotherm is the separation factor constant, R_L, which is given by Equation 3.

The Freundlich model is an empirical model based on multilayer adsorption and surface heterogeneity, the equation (4) [270].

The parameters calculated from the Freundlich and Langmuir models at three different temperatures are shown in Table 30.

Table 30. Parameters of the isotherms for the adsorption of Sb (III) on ox-xGnP

T (K)	Freundlich Isotherm				Langmuir Isotherm			
	Parameters of isotherm			Performance parameter	Parameters of isotherm			Performance parameter
	K_F	n	1/n	R^2	K_L (L mg^{-1})	q_m (mg g^{-1})	R_L	R^2
T=293	9,66	1,45	0,69	0,965	1,04	18,2	0,49	0,994
T=298	8,88	1,51	0,66	0,965	1,23	15,3	0,45	0,989
T=303	4,66	1,50	0,66	0,849	1,36	7,65	0,42	0,923

Figure 29 shows the Freundlich and Langmuir adsorption isotherms of Sb (III) on ox-xGnP at temperatures of 293 K, 298 K, and 303 K.

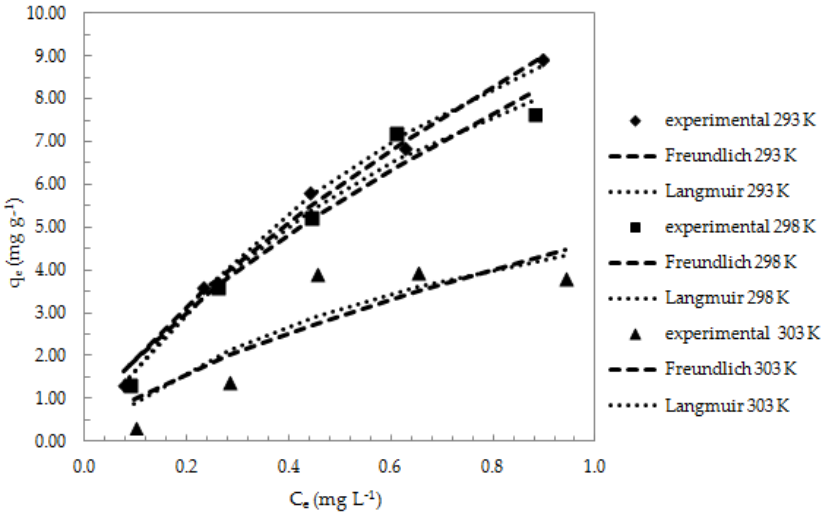

Figura 29. Non-linear Freundlich and Langmuir isotherms of Sb (III) adsorption on ox-xGnP (pH = 7.0, 1 mg L^{-1} Sb (III), 1 mg ox-xGnP/100 mL solution, T = 293 K, 298 K, 303 K, contact time 25 min)

The criterion for selecting the isotherm that best fits the experimental data is R^2. The values presented in Table 3 indicate that the Langmuir model best fit the experimental data at isothermal equilibrium. According to this model, the adsorption of Sb (III) on ox-xGnP was performed on homogeneous surfaces in monolayer. The maximum adsorption capacity at 293 K calculated from the Langmuir isotherm was q_m = 18.2 mg g^{-1} versus q_{exp} = 8.91 mg g^{-1}. The R_L values obtained for the three temperatures presented in Table 3 were between 0.42 and 0.49, which confirms that the adsorption of Sb (III) on ox-xGnP is favorable.

5.7. Thermodynamic study

In this study, the thermodynamic parameters associated with the adsorption process were also calculated, giving information about the type of interactions taking place. The thermodynamic parameters, namely, Gibb's free energy (ΔG^0, kJ mol^{-1}), enthalpy (ΔH^0, kJ mol^{-1}), and entropy (ΔS^0, J $mol^{-1}K^{-1}$), could provide data on the size of the adsorption process changing the internal energy throughout it. The parameters were determined by the following equations [271]:

$$\Delta G^0 = \Delta H^0 - T\Delta S^0 \quad (32)$$

$$\Delta G^0 = -RT \ln K_L \quad (33)$$

Based on Equations 32 și 33, Equations 34 and 35 are obtained:

$$\Delta H^0 - T\Delta S^0 = -RT \ln K_L \quad (34)$$

$$\ln(K) = \frac{\Delta S^0}{R} - \frac{\Delta H^0}{R} \cdot \frac{1}{T} \quad (35)$$

where:

K_L is the Langmuir equilibrium constant (L mol^{-1}), R is the gas constant (8.314 × 10^{-3} kJ mol^{-1}), T is the absolute temperature (K), ΔH^0 is the enthalpy (ΔH^0, kJ mol^{-1}), and ΔS^0 is the entropy (ΔS^0, J $mol^{-1}K^{-1}$). ΔH^0 and ΔS^0 are determined from the slope and the intercept of the linear fit of the van't Hoff plot, e.g., ln K_L versus 1/T (Figure 30). The calculated values are presented in Table 32.

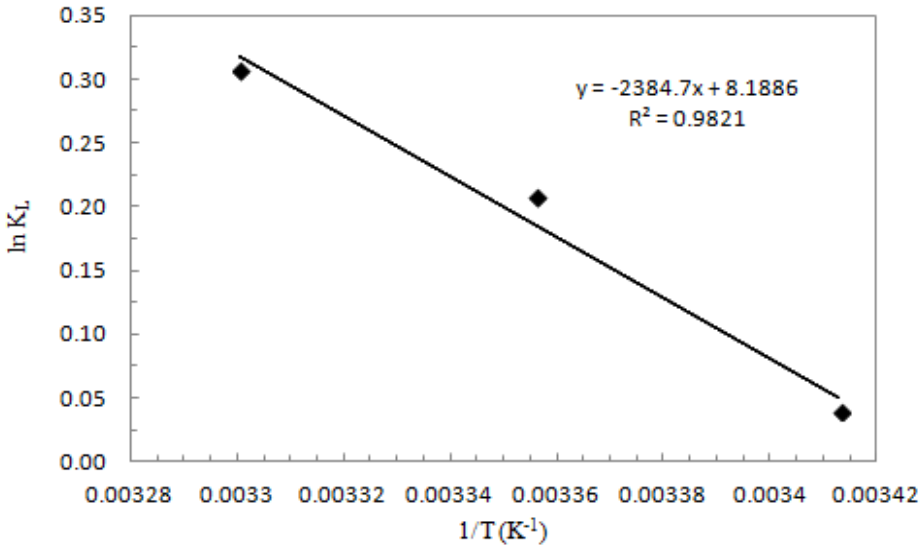

Figura 30. van't Hoff plot for the adsorption of Sb (III) onto ox-xGnP

Table 31. Thermodynamic parameters of Sb (III) adsorption on ox-xGnP. ΔH^0: enthalpy, ΔS^0: entropy, ΔG^0: Gibbs free energy.

ΔH^0 (kJ mol^{-1})	ΔS^0 (kJ mol^{-1} K^{-1})	ΔG^0 (kJ mol^{-1})		
		T=293 (K)	T=298 (K)	T=303 (K)
-19,8	0,068	-39,8	-40,1	-40,5

The negative value of ΔG^0 indicated that the adsorption process of Sb (III) on ox-xGnP was spontaneous and thermodynamically favored, the adsorbate having a high affinity for the adsorbent. The negative value of ΔH^0 indicated that the process was exothermic. That was also confirmed by the decrease of K_L with temperature. The positive value of ΔS^0 obtained from the adsorption process data suggested randomness at the solid–solution interface during the adsorption of Sb (III) on ox-xGnP and also the possibility of structural changes or readjustments in the adsorbate–adsorbent complex [271,272].

5.8. Proposed mechanism for adorption of Sb (III) onto ox-xGnP

To determine the adsorption mechanism, the following results of the studies were considered:

(1) The adsorption model was Langmuir-type, which means that the active centers on the ox-xGnP surface were the same, evenly distributed and did not influence each other;

(2) On the basis of literature data [277], the active species in the solution at pH = 7 was antimonous acid, $Sb(OH)_3$ [253], and the active positions on the ox-xGnP surface were –COO, as emphasized by the FT-IR analysis.

The mechanism (Figure 31) was formulated as follows:

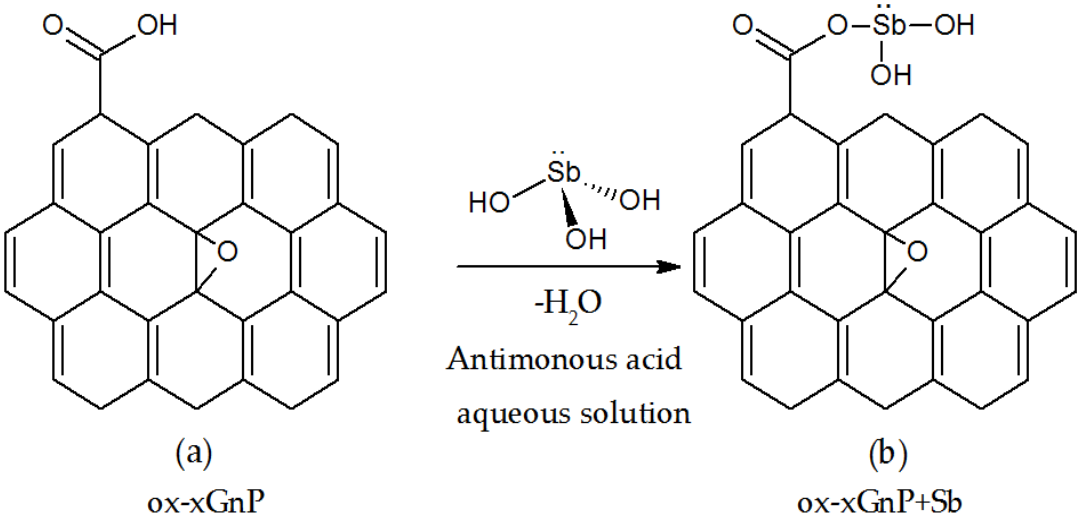

Figure 31. Proposed mechanism for adsorption of Sb (III) on ox-xGnP, (**a**) ox-xGnP, (**b**) ox-xGnP + Sb

The uniformity of distribution of active sites on the ox-xGnP surface was demonstrated by the SEM image (Figure 23b). The fact that the active species of Sb (III) was $Sb(OH)_3$ was supported by both the STEM and EDX analyses on one hand (Figure 24b,c), which revealed the presence of Sb, and the negative zeta potential values and increased adsorption capacity at higher pH on the other hand. Stabilization of the tetrahedral adsorbed ion was visible in the SEM image (Figure 23d).

5.10. Environmental applications

To use ox-xGnP as an adsorbent to remove Sb (III) from different waters contaminated with this metal, the adsorption capacity was studied on real samples. The studies included the analysis of several types of waters presented in Tables 33 and 34.

The samples presented in Table 33 were fortified with 0.7 mg of L-1Sb (III) because the measured Sb concentration was below the limit of quantification of the ICP-OES method. Table 33 presents the characteristics of the samples studied.

Table 33. Presentation of water samples.

Parameters	Water samples /Chemical composition			
	Non - carbonated mineral water, supermarket	Carbonated mineral water forte, supermarket	Tap water, our laboratory	Surface Water, Bipea MR
pH	7,40±0,04	6,89±0,04	7,69±0,04	7,90±0,04
Conductivity (µS/cm)	492±1,0	1766±1,0	425±1,0	622±1,0
Ca^{2+} (mg L^{-1})	61,1±0,46	131±0,51	57,8±0,42	92,6±0,35
Mg^{2+} (mg L^{-1})	27,6±0,40	31,1±0,45	6,25±0,38	12,5±0,25
Na^{+} (mg L^{-1})	2,80±0,31	168±1,53	11,8±0,20	2,49±0,27
K^{+} (mg L^{-1})	0,417±0,02	2,38±0,31	2,31±0,25	2,49±0,26
Cl^{-} (mg L^{-1})	2,83±0,18	< 1,4*	26,9±0,67	28,4±0,60
SO_4^{2-} (mg L^{-1})	22,2±0,40	0,28±0,01	34,6±0,56	65,8±0,70
HCO_3^{-} (g L^{-1})	0,34±0,02	1,04±0,05	0,084±0,003	0,084±0,003

* The value represents the limit of quantification of the method

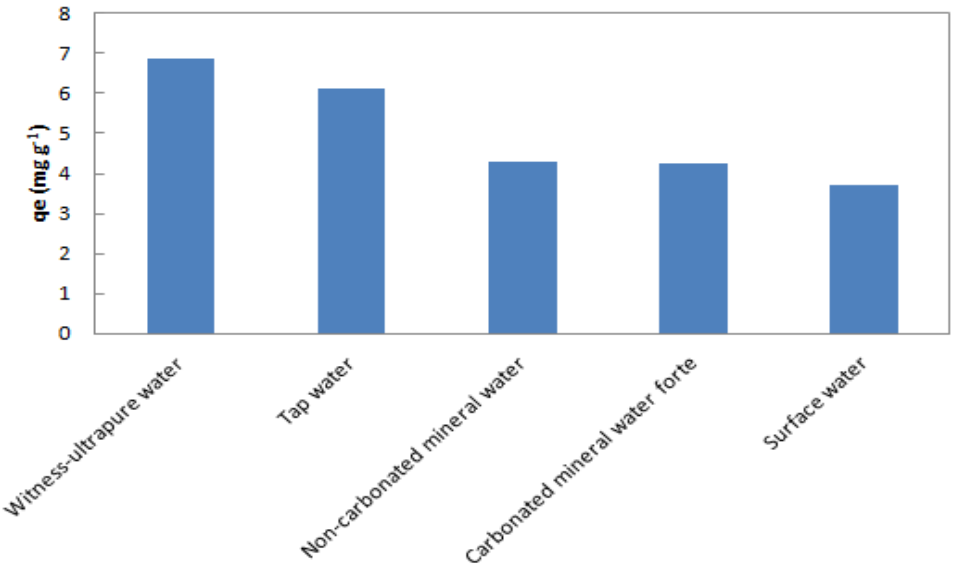

Figure 32. The adsorption capacity for Sb (III) from different real samples by ox-xGnP (pH=7.0, 0,7 mg L^{-1} Sb (III), 1 mg ox-xGnP/100 mL solution, T=293 K, contact time 25 minutes)

From Figure 32, we can see that the highest adsorption capacity of Sb (III) (6.86 mg g^{-1}) was obtained for ultrapure water and the lowest for surface water (3.70 mg g^{-1}). For tap water, the adsorption capacity of Sb (III) was 6.14 mg g^{-1}, followed by the adsorption capacity of Sb (III) for non-carbonated mineral water (4.30 mg g^{-1}) and carbonated mineral water forte (4.24 mg g^{-1}). The adsorption capacity of Sb (III) from tap water was the closest to the value for ultrapure water, due to the low content of bivalent cations (Ca^{2+} și Mg^{2+}) and organic pollutants, which is also confirmed by the low conductivity shown in Table 33. Smaller Sb (III) adsorption capacity for other water samples is justified by the presence of bivalent cations (Ca^{2+} și Mg^{2+}) that can compete with the analyte of interest for occupying active positions on the ox-xGnP surface [280,281]. In the case of surface water, the lower adsorption capacity compared to other types of water could be justified by the presence of bivalent cations of organic pollutants.

The presence of cations in this case resulted in an approximately 50% decrease in the adsorption capacity of Sb (III) in surface water compared to ultrapure water [280].

The adsorption capacity of Sb (III) using ox-xGnP was also tested on three samples of 90 g L^{-1} Na salt, whose chemical composition is shown in Table 34. Samples were processed according to the head. 5.2.3. The antimony concentration determined in the three samples was between 0.138-0.289 mg L^{-1}.

Table 34. Presentation of saline water samples.

Parameters	Saline water samples / Chemical composition		
	P 1	P 2	P 3
pH	10,1±0,04	10,1±0,04	10,1±0,04
Conductivity (µS/cm)	139,0±1,0	138,9±1,0	138,8±1,0
Sb (mg L^{-1})	0,246±0,06	0,289±0,06	0,138±0,06
Ca^{2+} % (v/v)	4,90±0,01	11,1±0,01	9,40±0,01
Mg^{2+} (mg L^{-1})	1,92±0,01	2,90±0,01	2,83±0,01
P % (v/v)	1,24±0,01	1,00±0,01	1,13±0,01
K^{+} % (v/v)	2,89±0,01	0,18±0,01	0,21±0,04
Cl^{-} % (v/v)	3,28±0,08	1,72±0,06	1,91±0,06
SO_4^{2-} % (v/v)	2,25±0,13	0,79±0,08	0,97±0,09

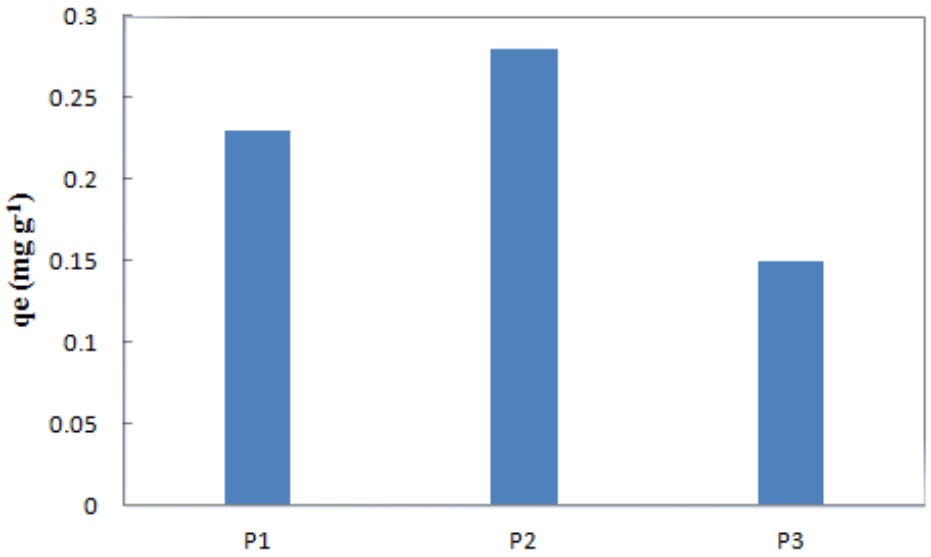

Figure 33. Adsorption capacity of Sb (III) from saline water samples
(pH=7,0, 1 mg ox-xGnP/100 mL solution, T=293 K, contact time 25 minutes)

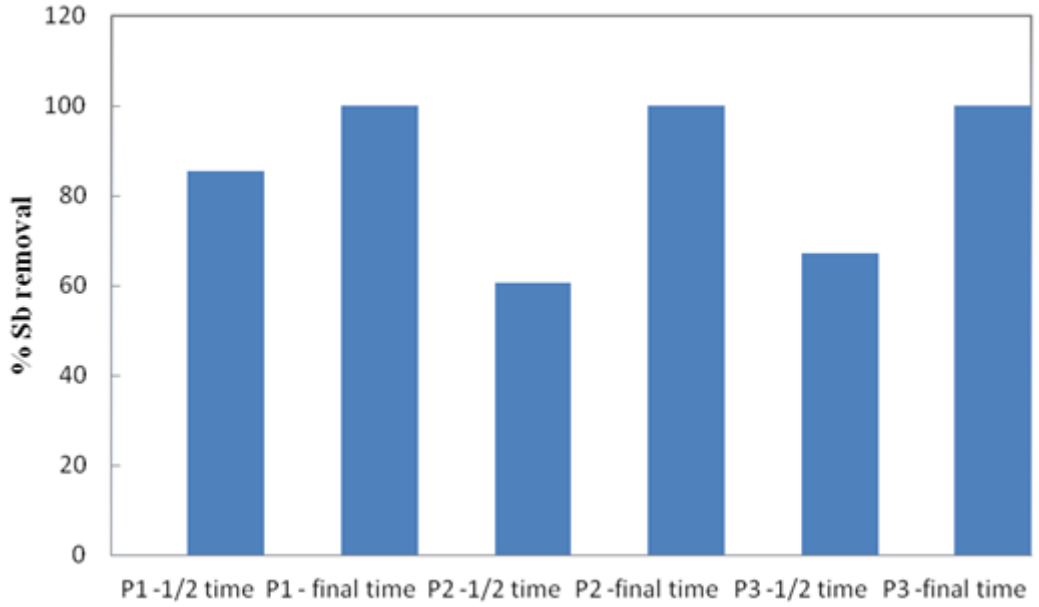

Figure 34. Rate of removal of Sb (III) from saline water samples
(pH=7,0, 1 mg ox-xGnP/100 mL solution, T=293 K, contact time 25 minutes)

From the data obtained, shown in Figures 33 and 34, it was observed that at half-time the removal rate was 60-80%, as at the end of the contact time, the removal rate of Sb was 100% for all the three samples. The adsorption capacities for the three samples are correlated with the concentration of Sb present in the three samples.

Conclusions

In this paper, Sb (III) adsorption was evaluated by using ox-xGnP as an adsorbent. The ox-xGnP was characterized by TGA, FT-IR, BET, SEM, and TEM analysis techniques. To optimize the adsorption process, several parameters were studied, namely, the influence of pH, the influence of the ox-xGnP concentration, the influence of the contact time, the influence of the initial concentration of Sb (III), and the temperature. The study of these parameters revealed the best adsorption capacity of Sb (III) on ox-xGnP at pH = 7.0, with 1.0 mg ox-xGnP/100 mL solution, T = 293 K, 1.0 mg L^{-1} Sb (III), contact time 25 min. The results of Sb (III) adsorption on ox-xGnP showed that the best correlation of kinetic data was described by the pseudo-first-order kinetic model. The adsorption isotherms of Sb (III) onto ox-xGnP were better described by the Langmuir isotherm model than by the Freundlich isotherm. The maximum adsorption capacity obtained from the Langmuir isotherm was 18.2 mg g^{-1}. The thermodynamic parameters studied showed that the adsorption process of Sb (III) on ox-xGnP was exothermic and spontaneous.

Sb (III) adsorption capacity was studied on ox-xGnP in different water samples, and the results obtained demonstrated the influence of Ca^{2+} and Mg^{2+} bivalent cations on the sorption capacity of Sb (III) on ox-xGnP, which determined a decreasing the adsorption capacity of Sb (III) for water samples where their concentrations were higher compared to other samples where the concentrations were lower, as well as the experimental conditions and the matrix of the analyzed samples.

Also, an Sb (III) adsorption mechanism on ox-xGnP was proposed based on experimental data that identified active positions on the x-xGnP surface by FT-IR analysis as -COO and based on of the literature data indicating that the active species of Sb (III) is $Sb(OH)_3$ at pH=7. The proposed mechanism is also supported by the SEM, STEM / EDX and potential zeta analyzes.

CHAPTER 6

6.1 GENERAL CONCLUSIONS

In order to achieve the proposed aim - the study of Sb (III) adsorption on oxidized exfoliated nanoplatelets graphite (ox-xGnP) in order to evaluate the potential of ox-xGnP as an adsorbent for Sb (III), the research activities undertaken within the doctoral thesis had the following results:

1. A method for the determination of Sb in drinking water (tap water) in the concentration range of 2-30 μg L^{-1} by inductively coupled plasma optical (ICP-OES) spectrometry was developed and validated using the Optima 2100 instrument DV ICP-OES System Perkin Elmer (Waltham, Ma, USA). The optimal parameters of the developed method are as follows: for linearity, correlation coefficient r=0.9992, the limit of detection, LoD=1.14 μg L^{-1} and the limit of quantification, LoQ = 3.42 μg L-1 . The repeatability value obtained was s_r = 0.55 μg L^{-1}, the accuracy value also was δ=0.31 μg L^{-1}, and the recovery was 103%. The extended uncertainty value was 1.7 μg L^{-1} with a confidence level of 95% (k=2). In the absence of an inter-laboratory study for determination of the performance of the method, the composed uncertainty gives a reasonable estimation of reproducibility.
2. A precise analytical method for the determination of Sb in natural mineral water with direct analysis of mineral water samples has been developed and validated. It represents a simple, cheap and fast measurement, characterized by high recovery at low concentration of Sb determined from carbonated mineral water, by ICP-OES technique. Over the studied concentration range, of 2-20 μg L^{-1}, the slope of the calibration curve, expressed through correlation coefficient r=0.9992, the detection limits LoD=0.67 μg L^{-1} and quantification LoQ=2.01 μg L^{-1}, a value of 0.25 μg L^{-1} for the standard repeatability deviation (sr), the accuracy of δ=0.16 μg L^{-1} and the 102% recovery, satisfy the acceptance criteria required by the legislation in force. The expanded uncertainty value with a confidence level of 95% (k=2) is 1.0 μg L^{-1} obtained for the Sb concentration = 4.10 μg L^{-1}.
3. The standard addition method (SAM) for comparative analysis of carbonated mineral waters with the calibration curve method (CCM) has been developed and optimized. The correlation coefficients of the calibration curves obtained by the method of standard additions ranged between r=0.9990 and r=0.9999. The concentration of Sb in the analyzed mineral waters is below the detection limit (LoD) of the calibration curve

method (CCM) developed method. The standard addition method (SAM) offering some great advantages regarding the matrix interferences and decreasing the limit of detection from 0.67 to 0.16 μg L^{-1}.

4. A simple, inexpensive cheap and quick way of antimony method in the range of 10-500 mg Kg-1 has been developed to determine the PET sting based on an original digestion method coupled with the ICP-OES measurement technique. The digestion method, developed and optimized for this study, uses only one digestion reagent (HNO_3), in comparison with other methods presented in the literature and shorter digestion time, too. The reagent is friendly to the measurement equipment, ensures a reduced digestion time (45 min.), thus having small energy consumption (0.15KWh/sample) and requesting standard digestion equipment. On the studied concentration range, the calibration curve slope, expressed through correlation coefficient r = 0.9999, standard deviation of repeatability of 1.27 mg Kg^{-1}, RSD = 0.49 %, accuracy determined by recovery degree ranges between 85 % and 96 % satisfy the demands of chemists for these parameters, being comparable with literature data. The value of extended uncertainty is 8.4 mg Kg^{-1} with a confidence level of 95 % (k=2), obtained for Sb content of 260 mg Kg^{-1}.
5. Oxidized exfoliated nanoplatelets graphite (ox-xGnP) was characterized by TGA, FT-IR, BET, SEM and TEM STEM / EDX analysis techniques before and after adsorption of Sb.
6. To optimize the adsorption process, several parameters were studied, namely:
   - the influence of pH solutions in the pH range of 4.0-11.0;
   - the influence of ox-xGnP concentration between 1.0-2.0 mg;
   - the influence of contact time;
   - the influence of the initial concentration of Sb (III) between 0.1-1.0 mg L^{-1};
   - and the temperature influence between 20°C-30°C.

   The study of these parameters revealed the best adsorption capacity of Sb (III) on ox-xGnP at pH = 7.0, with 1.0 mg ox-xGnP/100 mL solution, T=293 K, 1.0 mg L^{-1} Sb (III), contact time 25 min.
7. The kinetics of the adsorption process were studied on the basis of three kinetic models: the order I kinetic model, the order II kinetic model, and the intra-particle diffusion. The results of Sb (III) adsorption on ox-xGnP showed that the best correlation of kinetic data was described by the pseudo-first-order kinetic model.
8. The study of Sb (III) adsorption isotherms on ox-xGnP were described by two models: the Langmuir isotherm model and the Freundlich isotherm model. The value of the determination coefficient, R^2 showed that the Langmuir model best fits the experimental data to isothermal equilibrium, the adsorption of Sb (III) on ox-xGnP being performed on

homogeneous surfaces in the monolayer. The maximum adsorption capacity obtained from the Langmuir isotherm was 18.2 mg g^{-1}.

9. Thermodynamic parameters were also studied: Gibbs free energy (ΔG^0, kJ mol^{-1}), enthalpy (ΔH^0, kJ mol^{-1}) and entropy (ΔS^0, J $mol^{-1}K^{-1}$), which showed that the adsorption process of Sb (III) on ox-xGnP is exothermic and spontaneous. The positive value of ΔS^0 obtained from the adsorption process data suggested randomness at the solid–solution interface during the adsorption of Sb (III) on ox-xGnP and also the possibility of structural changes or readjustments in the adsorbate–adsorbent complex.
10. Sb (III) adsorption capacity was studied on ox-xGnP in different water samples, and the results obtained demonstrated the influence of Ca^{2+} and Mg^{2+} bivalent cations on the sorption capacity of Sb (III) on ox-xGnP, which determined a decreasing the adsorption capacity of Sb (III) for water samples where their concentrations were higher compared to other samples where the concentrations were lower, as well as the experimental conditions and the matrix of the analyzed samples.
11. Also, an Sb (III) adsorption mechanism on ox-xGnP was proposed based on experimental data that identified active positions on the x-xGnP surface by FT-IR analysis as -COO and based on of the literature data indicating that the active species of Sb (III) is $Sb(OH)_3$ at pH=7. The proposed mechanism is also supported by the SEM, STEM / EDX and potential zeta analyzes.

6.2. ORIGINALITY OF THESIS

The original aspects of the doctoral thesis are presented below:

- development of analysis methods for Sb analysis of drinking and mineral waters;
- development of an original method of digestion of PET;
- development of a method of determining Sb in PET;
- using ox-xGnP for the first time in the study of adsorption Sb (III);
- proposing a mechanism of adsorption of Sb (III) on ox-xGnP.

6. 3. FUTURE RESEARCH DIRECTIONS

The experimental results of the studies elaborated within this thesis open up future research directions, among which we can list:

- research studies on the migration of Sb from PET into various beverages;
- comparative studies of competitive adsorption of compounds present in water;
- sorption studies using microbic sorbents containing the used nanostructures and other inorganic materials.

CHAPTER 7

DISSEMINATION OF RESEARCH RESULTS

7.1. Scientific activity during doctoral studies

Works published in ISI rated journals:

1. **Capră Luiza**, Manolache Mihaela, Ion Ion, Alina Catrinel Ion, Validation of a method for determination of antimony in drinking water by ICP-OES, *U.P.B.* Sci. Bull., Series B: Chemistry and Materials Science, 78, 2016, p.103.
2. **Luiza Capră**, Mihaela Manolache, Ion Ion, Elena Radu, Alina Catrinel Ion, The Optimization and Validation of a Method For Sb Determination From PET by ICP-OES, Rev.Chim., (Bucharest), 68, No. 9, 2017 (Factor Impact 1,412).
3. Ileana Rădulescu, Marian Romeo Calin, Ion Ion, Alina Catrinel Ion, **Luiza Capră**, C.A. Simion, Gross Alpha, Gross Beta and Gamma Activities In Bottled Natural Water From Romania, Romanian Reports in Physics 69, 710, 2017 (Factor Impact 1,582).
4. Florinela Sârbu, Alina Catrinel Ion, **Luiza Capră**, Ion Ion**,** Thermodynamics Study on the Tetrahydrofuran Effect in Exfoliated Graphite Nanoplatelets and Activated Carbon Mixtures at Temperatures Between 293.15 and 308.15k, Advances in Materials Science and Engineering, Hindawi, Volume 2018. (Factor Impact 1,372).
5. **Luiza Capră**, Mihaela Manolache, Ion Ion, Rusăndica Stoica, Alina Catrinel Ion, Validation and Optimization of a Method For Sb Determination From Bottled Natural Mineral Waters By ICP-OES, Rev.Chim. (Bucharest), 69, No. 8, 2018 (Factor Impact 1,412).
6. **Luiza Capră**, Mihaela Manolache, Ion Ion, Rusăndica Stoica, Gabriela Stîngă, Sanda Maria Doncea, Elvira Alexandrescu, Raluca Somoghi, Marian Romeo Calin, Ileana Rădulescu, Georgeta Ramona Ivan, Marian Deaconu, Alina Catrinel Ion, Adsorption of Sb (III) on Oxidized Exfoliated Graphite Nanoplatelets, Nanomaterials 2018, 8, 992; Doi:10.3390/Nano8120992, (Factor Impact 3,504).

Participations in conferences:

1. **Luiza Capră,** Mihaela Manolache, Ion Ion, Alina Catrinel Ion, Validation and optimization of a method for Sb determination from drinking water by ICP-OES, Simpozionul International PRIOCHEM ed.11, Octombrie, 2015, București, Romania.
2. **Luiza Capră,** Mihaela Manolache, Ion Ion, Rusăndica Stoica, Alina Catrinel Ion, Validation and optimization of a method for Sb determination from mineral waters by ICP-OES, 3 rd International Conference on Chemical Engineering, ROMANIA, Iasi, 9-11 november 2016.
3. **Luiza Capră**, Mihaela Manolache, Ion Ion, Rusăndica Stoica, Georgeta Ivan, Alina Catrinel Ion, Adsorption of Sb (III) on Exfoliated Graphite Nanoplatelets (xGnP), 20th Romanian International Conference on Chemistry and Chemical Engineering, RICCCE 2017, 6-9 September 2017, Poiana Brasov, Romania;

Selective references

3. Chowdhury, S.; Mazumder, M.A.J.; Al-Attas, O.; Husain, T. Heavy metals in drinking water: Occurrences, implications, and future needs in developing countries. *The Science of the total environment* **2016**, *569-570*, 476-488, doi:10.1016/j.scitotenv.2016.06.166.

4. Smichowski, P. Antimony in the environment as a global pollutant: a review on analytical methodologies for its determination in atmospheric aerosols. *Talanta* **2008**, *75*, 2-14.
89. Lu, J.; Drzal, L.T.; Worden, R.M.; Lee, I. Simple Fabrication of a Highly Sensitive Glucose Biosensor Using Enzymes Immobilized in Exfoliated Graphite Nanoplatelets Nafion Membrane. *Chem. Mat.* **2007**, *19*, 6240-6246, doi:10.1021/cm702133u.
100. Das, A.; Kasaliwal, G.R.; Jurk, R.; Boldt, R.; Fischer, D.; Stöckelhuber, K.W.; Heinrich, G. Rubber composites based on graphene nanoplatelets, expanded graphite, carbon nanotubes and their combination: a comparative study. *Composites Science and Technology* **2012**, *72*, 1961-1967.
109. Agnihotri, S.; Rostam-Abadi, M.; Rood, M.J. Temporal changes in nitrogen adsorption properties of single-walled carbon nanotubes. *Carbon* **2004**, *42*, 2699-2710.
111. Elmer, P. BOSS B. C., FREDEEN J. K., Concepts, Instrumentation and Techniques in Inductively Coupled Plasma Optical Emission Spectrometry, Perkin Elmer, USA, 2004, chapter 4, p. 6.
112. Wang, X.; Liu, B.; Lu, Q.; Qu, Q. Graphene-based materials: fabrication and application for adsorption in analytical chemistry. *Journal of chromatography. A* **2014**, *1362*, 1-15, doi:10.1016/j.chroma.2014.08.023.
119. Gupta, V.K.; Tyagi, I.; Sadegh, H.; Ghoshekand, R.S.; Makhlouf, A.S.H.; Maazinejad, B. Nanoparticles as Adsorbent; A Positive Approach for Removal of Noxious Metal Ions: A Review. *Science, Technology and Development* **2015**, *34*, 195-214, doi:10.3923/std.2015.195.214.
151. Langmuir, I. The adsorption of gases on plane surfaces of glass, mica and platinum. *Journal of the American Chemical society* **1918**, *40*, 1361-1403.
175. Law No. 458, (2002), on the quality drinking water modified and completed by Government Decision no. 22/2017, Romanian Official Monitor, 03th of September 2017
183. Council Directive 98/83/EC of 3 November 1998 on the quality of water intended for human consumption, Official Journal of the European Communities, L330, 32-54, amended by Commission Directive (EU) 2015/1787 of 6 Octomber 2015, L 260/66, 07.10.2015, Brussels.
206. De Jesus, A.; Dessuy, M.B.; Huber, C.S.; Zmozinski, A.V.; Duarte, Á.T.; Vale, M.G.R.; Andrade, J.B. Determination of antimony in pet containers by direct analysis of solid samples using graphite furnace atomic absorption spectrometry and leaching studies. *Microchemical Journal* **2016**, *124*, 222-227, doi:10.1016/j.microc.2015.08.016.
209. Capra, L.; Manolache, M.; Ion, I.; Ion, A.C. Validation of a Method For Determination of Antimony in Drinking Water by ICP-OES. *University Politehnica Of Bucharest Scientific Bulletin Series B-Chemistry And Materials Science* **2016**, *78*, 103-112.
210. Ion Gh. Tanase, Alexandru Pana, Gabriel Lucian Radu. Mihaela Buleandra, " Validarea metodelor analitice", Editura Printech, 2007.
211. SR EN ISO 11885/2009 - Water quality. Determination of selected elements by inductively coupled plasma optical emission spectromety (ICP -OES).
213. Cuantificarea incertitudinii de masurare in masurarea analitica" Ghid Eurachem/CITAC, Editia a II-a, Editura Ars Docendi, 2002.
214. Capra, L.; Manolache, M.; Ion, I.; Stoica, R.; Ion, A.C. Validation and Optimization of a Method for Sb Determination from Bottled Natural Mineral Waters by ICP-OES. *Revista de Chimie* **2018**, *69*, 2102-2106.
222. Keresztes, S.; Tatar, E.; Mihucz, V.G.; Virag, I.; Majdik, C.; Zaray, G. Leaching of antimony from polyethylene terephthalate (PET) bottles into mineral water. *The Science of the total environment* **2009**, *407*, 4731-4735, doi:10.1016/j.scitotenv.2009.04.025.
224. Sanchez-Martinez, M.; Perez-Corona, T.; Camara, C.; Madrid, Y. Migration of antimony from PET containers into regulated EU food simulants. *Food chemistry* **2013**, *141*, 816-822, doi:10.1016/j.foodchem.2013.03.067.

225. Hauswaldt, A.-L.; Rienitz, O.; Jährling, R.; Fischer, N.; Schiel, D.; Labarraque, G.; Magnusson, B. Uncertainty of standard addition experiments: a novel approach to include the uncertainty associated with the standard in the model equation. *Accreditation and Quality Assurance* **2012**, *17*, 129-138.
226. Capra, L.; Manolache, M.; Ion, I.; Radu, E.; Ion, A.C. The Optimization and Validation of a Method for Sb Determination from PET by ICP-OES. *Rev. Chim.(Bucharest)* **1969**, *68*.
227. Westerhoff, P.; Prapaipong, P.; Shock, E.; Hillaireau, A. Antimony leaching from polyethylene terephthalate (PET) plastic used for bottled drinking water. *Water research* **2008**, *42*, 551-556, doi:10.1016/j.watres.2007.07.048.
230. Lopez-Molinero, A.; Calatayud, P.; Sipiera, D.; Falcon, R.; Liñan, D.; Castillo, J.R. Determination of antimony in poly (ethylene terephthalate) by volatile bromide generation flame atomic absorption spectrometry. *Microchimica Acta* **2007**, *158*, 247-253.
231. Fan, Y.-Y.; Zheng, J.-L.; Ren, J.-H.; Luo, J.; Cui, X.-Y.; Ma, L.Q. Effects of storage temperature and duration on release of antimony and bisphenol A from polyethylene terephthalate drinking water bottles of China. *Environmental Pollution* **2014**, *192*, 113-120, doi:https://doi.org/10.1016/j.envpol.2014.05.012.
232. Carneado, S.; Hernández-Nataren, E.; López-Sánchez, J.F.; Sahuquillo, A. Migration of antimony from polyethylene terephthalate used in mineral water bottles. In *Food chemistry*, 2015; Vol. 166, pp 544-550.
233. Rungchang, S.; Numthuam, S.; Qiu, X.; Li, Y.; Satake, T. Diffusion coefficient of antimony leaching from polyethylene terephthalate bottles into beverages. *Journal of Food Engineering* **2013**, *115*, 322-329, doi:10.1016/j.jfoodeng.2012.10.025.
234. GmbH, A.P. Manual for Microwave digester Multiwave 3000, Anton Paar GmbH, Austria, 2006, p. 352.
235. Horwitz, W.; Kamps, L.R.; Boyer, K.W. Quality assurance in the analysis of foods and trace constituents. *Journal - Association of Official Analytical Chemists* **1980**, *63*, 1344-1354.
236. Capra, L.; Manolache, M.; Ion, I.; Stoica, R.; Stinga, G.; Doncea, S.M.; Alexandrescu, E.; Somoghi, R.; Calin, M.R.; Radulescu, I., et al. Adsorption of Sb (III) on Oxidized Exfoliated Graphite Nanoplatelets. *Nanomaterials (Basel)* **2018**, *8*, 992, doi:10.3390/nano8120992.
237. Ion, A.C.; Alpatova, A.; Ion, I.; Culetu, A. Study on phenol adsorption from aqueous solutions on exfoliated graphitic nanoplatelets. *Materials Science and Engineering: B* **2011**, *176*, 588-595.
238. Sirbu, F.; Ion, A.C.; Capra, L.; Ion, I. A Thermodynamics Study on the Tetrahydrofuran Effect in Exfoliated Graphite Nanoplatelets and Activated Carbon Mixtures at Temperatures between 293.15 and 308.15 K. *Advances in Materials Science and Engineering* **2018**, *2018*.
239. Ubarhande, S.S.; Burghate, A.S.; Berad, B.N.; Turak, J.D. Studies on refractive index of 1, 3-diaryl carbamides in different percentage of binary liquid mixture. *RASAYAN Journal of Chemistry* **2011**, *4*, 585-587.
243. Cho, H.-H.; Wepasnick, K.; Smith, B.A.; Bangash, F.K.; Fairbrother, D.H.; Ball, W.P. Sorption of aqueous Zn [II] and Cd [II] by multiwall carbon nanotubes: the relative roles of oxygen-containing functional groups and graphenic carbon. *Langmuir* **2009**, *26*, 967-981.
244. Choi, E.-Y.; Han, T.H.; Hong, J.; Kim, J.E.; Lee, S.H.; Kim, H.W.; Kim, S.O. Noncovalent functionalization of graphene with end-functional polymers. *Journal of Materials Chemistry* **2010**, *20*, 1907-1912.

246. Pan, M.; Wu, G.; Liu, C.; Lin, X.; Huang, X. Enhanced Adsorption of Zn (II) onto Graphene Oxides Investigated Using Batch and Modeling Techniques. *Nanomaterials* **2018**, *8*, 806.
247. Ghazaryan, V.V.; Fleck, M.; Petrosyan, A.M. Structure and vibrational spectra of L-alanine L-alaninium picrate monohydrate. *Journal of Molecular Structure* **2012**, *1015*, 51-55.
248. Vijayan, N.; Rajasekaran, S.; Bhagavannarayana, G.; Ramesh Babu, R.; Gopalakrishnan, R.; Palanichamy, M.; Ramasamy, P. Growth and characterization of nonlinear optical amino acid single crystal: L-alanine. *Crystal growth & design* **2006**, *6*, 2441-2445.
249. Merline, G.K.P.; Chitra, M. Investigation on optical, thermal, dielectric and mechanical properties of antimony potassium tartrate on l-alanine single crystals. *Journal of Materials Science: Materials in Electronics* **2018**, *29*, 5509-5517.
250. Reddy, J.R.; Ravi, G.; Suresh, P.; Veldurthi, N.K.; Velchuri, R.; Vithal, M. Antimony potassium tartrate. *Journal of Thermal Analysis and Calorimetry* **2014**, *115*, 1321-1327.
253. Constantino, L.V.; Quirino, J.N.; Abrão, T.; Parreira, P.S.; Urbano, A.; Santos, M.J. Sorption–desorption of antimony species onto calcined hydrotalcite: Surface structure and control of competitive anions. *Journal of hazardous materials* **2018**, *344*, 649-656.
254. Sarı, A.; Çıtak, D.; Tuzen, M. Equilibrium, thermodynamic and kinetic studies on adsorption of Sb (III) from aqueous solution using low-cost natural diatomite. *Chemical Engineering Journal* **2010**, *162*, 521-527.
266. Lagergren, S.K. About the theory of so-called adsorption of soluble substances. *Sven. Vetenskapsakad. Handingarl* **1898**, *24*, 1-39.
267. Rudzinski, W.; Panczyk, T. Remarks on the current state of adsorption kinetic theories for heterogeneous solid surfaces: a comparison of the ART and the SRT approaches. *Langmuir* **2002**, *18*, 439-449.
268. Rudzinski, W.; Plazinski, W. On the applicability of the pseudo-second order equation to represent the kinetics of adsorption at solid/solution interfaces: a theoretical analysis based on the statistical rate theory. *Adsorption* **2009**, *15*, 181.
269. Weber, W.J.; Morris, J.C. Kinetics of adsorption on carbon from solution. *Journal of the Sanitary Engineering Division* **1963**, *89*, 31-60.
270. Freundlich, H. Über die adsorption in lösungen. *Zeitschrift für physikalische Chemie* **1907**, *57*, 385-470.
271. Bergmann, C.P.; Machado, F.M. *Carbon nanomaterials as adsorbents for environmental and biological applications*; Springer: 2015.
272. Balarak, D. Kinetics, isotherm and thermodynamics studies on bisphenol A adsorption using barley husk. *International Journal of ChemTech Research* **2016**, *9*, 681-690.
273. Webb, P.A.; Orr, C. *Analytical methods in fine particle technology*; Micromeritics Instrument Corp: 1997.
277. Watkins, R.; Weiss, D.; Dubbin, W.; Peel, K.; Coles, B.; Arnold, T. Investigations into the kinetics and thermodynamics of Sb (III) adsorption on goethite (α-FeOOH). *Journal of colloid and interface science* **2006**, *303*, 639-646.
280. Simeonidis, K.; Martinez-Boubeta, C.; Zamora-Pérez, P.; Rivera-Gil, P.; Kaprara, E.; Kokkinos, E.; Mitrakas, M. Implementing nanoparticles for competitive drinking water purification. *Environmental Chemistry Letters* **2018**, 1-15.
281. Zhang, L.-q.; Zhang, Y.-k.; Lin, X.-c.; Yang, K.; Lin, D.-h. The role of humic acid in stabilizing fullerene (C 60) suspensions. *Journal of Zhejiang University SCIENCE A* **2014**, *15*, 634-642.